Pol. J. Environ. Stud. Vol. 30, No. 3 (2021), 2395-2436
DOI: *10.15244/pjoes/126501* ONLINE PUBLICATION DATE: 2021-01-29

Original Research

Dynamic Characterization of Combined Toxicity Interaction of Heavy Metals Towards *Chlorella pyrenoidosa*

Jin Zhang*, Tao Wang, Longke Ban, Zhiqiang Bian, Fakang Pan

Key Laboratory of Water Pollution Control and Wastewater Resource of Anhui Province, College of Environment and Energy Engineering, Anhui Jianzhu University, Hefei, China

Received: 23 February 2020
Accepted: 18 August 2020

Abstract

Typical contaminants heavy metals are threatening the survival and health of organisms in the aquatic ecosystem. Therefore, toxic effects and possible mechanisms of five heavy metals, copper (Cu), manganese (Mn), cadmium (Cd), zinc (Zn), lead (Pb), and their mixtures towards *Chlorella pyrenoidosa* (*C. pyrenoidosa*) were investigated by the time-dependent microplate toxicity analysis (t-MTA) method. Here, direct equilibration ray method (EquRay) and uniform design ray method (UD-Ray) were used to design ten binary and one quinary mixture systems, respectively. Then, a return-to-zero fitting (RTZF) method was used to analyze toxicity interaction within mixture systems. According to RTZF, one binary and quinary heavy metal mixture systems exhibit time-dependent and component-dependent antagonism. Antagonism in Zn-Cd mixture system increases gradually from 24 to 48 h then decreases gradually from 48 to 96 h. Toxicity interaction within quinary mixture changes from additive action to antagonism and to additive action again over time. The change of chlorophyll-a reduction rate under the action of different heavy metal is slightly different. The toxicity mechanism of copper on algal cells include destruction of cell membrane and chloroplast structure.

Keywords: heavy metals, *Chlorella pyrenoidosa*, toxicity interaction, mechanism

Introduction

Heavy metals are typical contaminants in the aquatic ecosystem [1-2]. According to published reports, aquatic environment of some coastal cities in China such as Songhua River and Jiaozhou Bay has been polluted by heavy metals, and the heavy-metal contents of urban sludge generally exceed the standard concentration [3-4]. Heavy-metal pollution is irreversible, complex, long-term, and even poses a direct threat to human health through food chains and food webs [5-7]. Heavy metals enter the human's body by eating agricultural products or aquatic products and cause obvious potential accumulation toxicity [8]. The damages resulted from heavy-metal pollution such as world-shocking incidents Minamata and Itai-itai disease in Japan are hard to estimate [9-10]. Therefore, it is of vital importance to precisely assess the environmental risks of heavy metals in the aquatic system.

*e-mail: ginnzy@163.com

As we all know, the heavy metals entering the environment will not exist in a single form but various forms and concentrations, thus more harmful mixed pollutants come into being [11]. Mixtures with multiple components at the no observed effect concentration (NOEC) or lower concentrations are also likely to cause significant toxicity even toxicity interaction such as synergism and antagonism to aquatic organisms [12]. Furthermore, higher toxicity towards the organisms can be observed by extending the exposure time of pollutants [13-14]. Therefore, study on the combined toxicity and dynamic characterization of toxicity interaction within mixtures is important for environmental risk assessment of heavy metal pollutions.

In addition, choosing an appropriate evaluation method is the key to accurately evaluate combined toxicity. Concentration addition (CA) and independent action (IA) are two common models to qualitatively evaluate the toxicity interaction within mixtures by comparing the observed concentration-response curves (CRCs) to those predicted curves by CA or IA. However, CA or IA cannot quantitatively assess the toxicity interaction intensity, and will have relatively larger prediction errors for the effects of the low concentration levels due to the larger uncertainty [15]. Therefore, a return-to-zero fitting method is introduced here to characterize toxicity interaction intuitively and quantitatively.

As stated above, this study aims to assess the potential risks of heavy metal pollution objectively and accurately, to quantitatively characterize the combined toxicity of heavy metals in different exposure time. Five heavy metals commonly found in the environment were selected as the mixture components, and *Chlorella pyrenoidosa* (*C. pyrenoidosa*) was used as the test organism. The direct equilibration ray method (EquRay) and uniform design ray method (UD-Ray) were used to design binary and quinary heavy metal mixtures, respectively. Toxicity data of heavy metals and their mixtures towards *C. pyrenoidosa* was determined using the time-dependent microplate toxicity analysis (t-MTA) method. Toxicity interactions in different exposure time were analyzed by the return-to-zero fitting (RTZF) method. The contents of chlorophyll-a in *C. pyrenoidosa* were determined, and the morphology of algal cells was observed by an electron microscope to preliminarily investigate the mechanism of heavy metals on *C. pyrenoidosa*. The obtained results will provide a data reference for scientific evaluation of environmental risk of heavy metal pollutants.

Materials and Methods

Chemicals

Five heavy metals, copper sulfate pentahydrate ($CuSO_4{\cdot}5H_2O$, Cu), manganese chloride tetrahedron ($MnCl_2{\cdot}4H_2O$, $MnCl_2$), zinc sulfate heptahydrate ($ZnSO_4{\cdot}7H_2O$, Zn), cadmium chloride ($CdCl_2{\cdot}2.5H_2O$, Cd), and lead chloride ($PbCl_2$, Pb) were purchased from Shanghai Yuanye Bio-technology Co., Ltd. (Shanghai, China). Their physi-chemical properties are given in Table 1. The stock solutions were prepared with Milli-Q water and stored in the dark at 4ºC.

Table 1. Basic physical properties of five heavy metals.

Component	Abbr.	CAS RN	MW [a]	Purity(%)
$CuSO_4{\cdot}5H_2O$	Cu	7758-99-8	249.69	≥99.0
$MnCl_2{\cdot}4H_2O$	Mn	13446-34-9	197.90	≥99.0
$ZnSO_4{\cdot}7H_2O$	Zn	7446-20-0	287.56	≥99.0
$CdCl_2{\cdot}2.5H_2O$	Cd	7790-78-5	228.35	≥99.0
$PbCl_2$	Pb	7758-95-4	278.11	≥99.0

[a] MW: molecular weight.

Experimental Organism and Toxicity Test

C. pyrenoidosa was purchased from Freshwater Algal Culture Collection at the Institute of Hydrobiology (FACHB). The manufacture of culture medium and cultivation of *C. pyrenoidosa* was the same as those reported in the literatures [16].

The growth of algae at different exposure time was determined by t-MTA. The inhibition I was used as the toxicity index to calculate the toxicity of five heavy metals and their mixtures on *C. pyrenoidosa*.

The formula for calculating the inhibition of *C. pyrenoidosa* is as follows:

$$I = \left(1 - \frac{OD}{OD_0}\right) \times 100\% \tag{1}$$

...where OD_0 is the average of optical density of *C. pyrenoidosa* exposed to the controls and OD is the average of optical density exposed to the tested chemicals.

Concentration-Response Curve Fitting

The experimental concentration-inhibition data in different exposure times were fitted nonlinearly by using APTox (Assessment and Prediction for the Toxicity of chemical mixtures) software procedure. The data was fitted to non-linear functions, namely, Logit. The goodness of fitting was characterized by the correlation coefficient (R^2) and root mean square error (RMSE). Considering the errors in toxicity experiment may reduce the accuracy of experimental data, the observed confidence interval (OCI) was applied to characterize the accuracy of toxicity data.

The Logit function can be written as follows:

$$E = 1 \big/ \left[1 + \exp\left(-\alpha - \beta \times \lg c \right) \right] \tag{2}$$

...where α and β are the parameters of position and slope of Logit, E is the effect that refers to the inhibition of chemicals on *C. pyrenoidosa* and c is the concentration of chemicals.

Mixture Design

In order to study the combined toxicity of simple mixtures, ten groups of binary mixture systems were designed by the EquRay method [17]. In order to simulate the actual environment as much as possible, a quinary mixture system was designed by the UD-Ray method to initially study the combined toxicity of complex mixtures [18]. The compositions and concentration ratio p_is of each mixture ray were listed in Table 2.

Characterization of Toxicity Interaction

Traditional CRC Comparison

Additive reference model can be used to analyze toxicity interaction within mixtures. Considering heavy metals with similar toxicity mechanism, CA model was chosen as the additive reference model to analyze the toxicity interaction within mixture rays [19-20].

CA model is as follows:

$$\sum_{i=1}^{n} \frac{C_i}{EC_{\chi,i}} = 1 \tag{3}$$

...where c_i is the concentration of component (i) in the mixture whose effect is x% and $EC_{x,i}$ is the concentration of the ith component at the combined effect of x%. If the observed toxicity of a mixture is consistent with the predicted toxicity of the model, greater or less than the predicted toxicity, the toxicity interactions are additive, synergism or antagonism, respectively [21].

Return-to-Zero Fitting Method

In order to reduce discriminant error, toxicity effects can be zeroed based on CRCs, so that the effects of each concentration level are normalized to the same scale. The method can also quantitatively assess the intensity of toxicity interaction, and the greater the distance from confidence intervals, the stronger the toxicity interaction intensity. The return-to-zero fitting (RTZF) method shows the changes of the effect differences at different concentrations of mixtures, and

Table 2. Composition and concentration ratio (pi) of heavy metal mixture systems.

Ray	P_{Zn}	P_{Mn}	Ray	P_{Zn}	P_{Pb}	Ray	P_{Zn}	P_{Cd}	Ray	P_{Zn}	P_{Cu}
R1	8.14E-01	1.86E-01	R1	1.28E-01	8.72E-01	R1	8.14E-01	1.86E-01	R1	9.09E-01	9.13E-02
R2	6.36E-01	3.64E-01	R2	5.54E-02	9.45E-01	R2	6.36E-01	3.64E-01	R2	7.99E-01	2.01E-01
R3	4.67E-01	5.33E-01	R3	2.85E-02	9.72E-01	R3	4.67E-01	5.33E-01	R3	6.66E-01	3.34E-01
R4	3.04E-01	6.96E-01	R4	1.44E-02	9.86E-01	R4	3.04E-01	6.96E-01	R4	4.99E-01	5.01E-01
R5	1.49E-01	8.51E-01	R5	5.83E-03	9.94E-01	R5	1.49E-01	8.51E-01	R5	2.85E-01	7.15E-01
Ray	P_{Mn}	P_{Cu}	Ray	P_{Pb}	P_{Cu}	Ray	P_{Cd}	P_{Cu}	Ray	P_{Mn}	P_{Cu}
R1	9.97E-01	2.86E-03	R1	9.97E-01	2.94E-03	R1	9.19E-01	8.08E-02	R1	9.97E-01	2.86E-03
R2	9.93E-01	7.13E-03	R2	9.93E-01	7.31E-03	R2	8.20E-01	1.80E-01	R2	9.93E-01	7.13E-03
R3	9.86E-01	1.42E-02	R3	9.86E-01	1.45E-02	R3	6.95E-01	3.05E-01	R3	9.86E-01	1.42E-02
R4	9.72E-01	2.79E-02	R4	9.71E-01	2.86E-02	R4	5.32E-01	4.68E-01	R4	9.72E-01	2.79E-02
R5	9.33E-01	6.70E-02	R5	9.31E-01	6.86E-02	R5	3.13E-01	6.87E-01	R5	9.33E-01	6.70E-02
Ray	P_{Pb}	P_{Cd}	Ray	P_{Pb}	P_{Mn}	Ray	P_{Pb}	P_{Zn}	P_{Cd}	P_{Cu}	P_{Mn}
R1	9.93E-01	6.66E-03	R1	8.30E-01	1.70E-01	R1	1.90E-01	8.19E-04	4.30E-03	6.03E-03	7.99E-01
R2	9.84E-01	1.65E-02	R2	6.61E-01	3.39E-01	R2	3.91E-01	9.09E-03	3.75E-02	1.77E-03	5.60E-01
R3	9.68E-01	3.24E-02	R3	4.94E-01	5.06E-01	R3	6.56E-01	3.73E-02	2.44E-03	1.38E-02	2.91E-01
R4	9.37E-01	6.28E-02	R4	3.28E-01	6.72E-01	R4	8.57E-01	4.36E-04	2.55E-02	3.57E-03	1.13E-01
R5	8.56E-01	1.44E-01	R5	1.63E-01	8.37E-01	R5	9.54E-01	4.15E-03	8.43E-04	1.70E-02	2.42E-02
						R6	9.64E-01	1.53E-02	1.07E-02	4.95E-03	5.37E-03
						R7	3.52E-01	1.57E-02	1.65E-02	5.83E-03	6.10E-01

the effect values of horizontal line is zero. The additive area exists between the upper and lower limits of the confidence interval, the antagonism area is above the upper limits of confidence interval, and the synergism area is below the lower limits [15].

Determination of Chlorophyll-a Content in *C. pyrenoidosa*

The toxic effects of heavy metals on algae are mainly manifested in the inhibition of cell division, growth rate, enzyme activity and photosynthesis efficiency [22]. Chloroplast is an important organelle in algal cells, which plays a key role in the light absorption of photosynthesis. *C. pyrenoidosa*, as an efficient photosynthetic autotroph, its chlorophyll content can be used not only to judge the photosynthetic physiological ability and growth of algae, but also as an important indicator to reflect the state of algae under environmental stress [23-24]. Chlorophyll-a is an important part of the complex weight of light harvesting pigment, which is more sensitive to pollutants than other photosynthetic pigments [25]. In this study, chlorophyll-a content was selected as the index to investigate the toxicity effect at different exposure time and concentrations to preliminarily explore the toxicity mechanism of heavy metal contaminants to *C pyrenoidosa*. Chlorophyll-a contents of *C. pyrenoidosa* at our effect concentrations (EC_{10}, EC_{30}, EC_{50}, and EC_{70}) were determined in 48 and 96 h. Analysis method of chlorophyll-a is detailed in the references [26-28].

Scanning of Cell Morphology of *C. pyrenoidosa*

The morphology of algal cells was observed by SEM, to determine the damage degree of heavy metal pollutants more intuitively to *C. pyrenoidosa* membrane. The morphological effects of heavy metal Cu were determined in cells exposed to EC_{30} and EC_{70} and compared to the control cells in the exposure time of 24, 48 and 96 h. The pretreatment methods of algal cells were described in the listed references [29-30]. SEM observations were made using a JEOL JSM-7500F scanning electron microscope, with an acceleration voltage of 5 kV.

Results and Discussion

Toxicity Interaction within Binary Mixture

The concentration-effect data of five heavy metals and their binary mixtures in different exposure time to *C. pyrenoidosa* can be well fitted by Logit function. The fitted location parameter (α) and shape parameter (β), statistical parameters (correlation coefficient (R) and root mean square error (RMSE) and negative logarithm of median effective concentration (pEC_{50})) are listed in Tables S1-11.

The EquRay method was used to design 10 binary mixture systems of five heavy metals, the combined toxicity in different exposure time was predicted by CA model, and the RTZF method was used to quantitatively characterize the toxicity interaction. By comparing the fitted CRCs and CA curves of 10 binary mixture systems, it was found that the toxicity interaction of Zn-Cd mixture system exposed for more than 24 h showed antagonism, and other mixture systems showed additive action. The RTZF curves of representative rays in Zn-Cd binary mixture system were shown in Fig. 1, the remaining rays' RTZF curves can be seen in Figs S1-10.

As shown in Fig. 1, RTZF curves locate in the 95% OCI in 12 h. These curves are partly within 95% OCI and the rest of curves are above 95% OCI in 24 h. The toxicity interaction from 12 to 24 h changes from additive action to partial antagonism. After 48 h, the RTZF curve is basically above the 95% OCI, showing clear antagonism. The antagonism within the Zn-Cd mixture system increases gradually from 24 to 48 h with RTZF value even approaches 0.4, and then decreases gradually from 48 h to 96 h.

It is generally believed that the antagonism of heavy metal mixtures in aquatic organisms is the result of competitive binding mechanism of biological ligands [31-32]. Heavy metal Cd and Zn have similar chemical properties and have been shown to compete for absorption in various tissues [33-35], which is consistent with our results. Meanwhile, Liu et al [19] noted that the mode of action of chemicals changes with concentration and time, i.e. the same mixture exhibits different types of combined toxicity in different concentration regions and exposure times. In this study, Zn-Cd binary mixture had the strongest antagonism in 48 h exposure in the medium concentration area. The reason why the antagonism only occurred in the binary mixture of Zn-Cd, and did not occur in other binary mixture systems, is a question in need of further research to clearly explain.

Toxicity Interaction within Quinary Mixture

The concentration-effect data of quinary mixture in different exposure time to *C. pyrenoidosa* can be well fitted by Logit function. The fitting results are shown in Table S12. Since the similar change regular of combined toxicity of seven rays in the quinary mixture system, the RTZF curves of three representative rays in quinary mixture system were shown in Fig. 2, other ones of the remaining rays can be seen in Fig S11.

Fig. 2 shows that RTZF curves in the whole concentration region are within the 95% OCI in 12 h, and the combined toxicity appears additive action. The RTZF curves are generally above the upper confidence limits when exposed in 24~48 h, indicating that the quinary mixture appears as an additive action in the low concentration region and a strong antagonism in the remaining region with RTZF value even approaching 0.4. Interestingly, the RTZF curves locate within

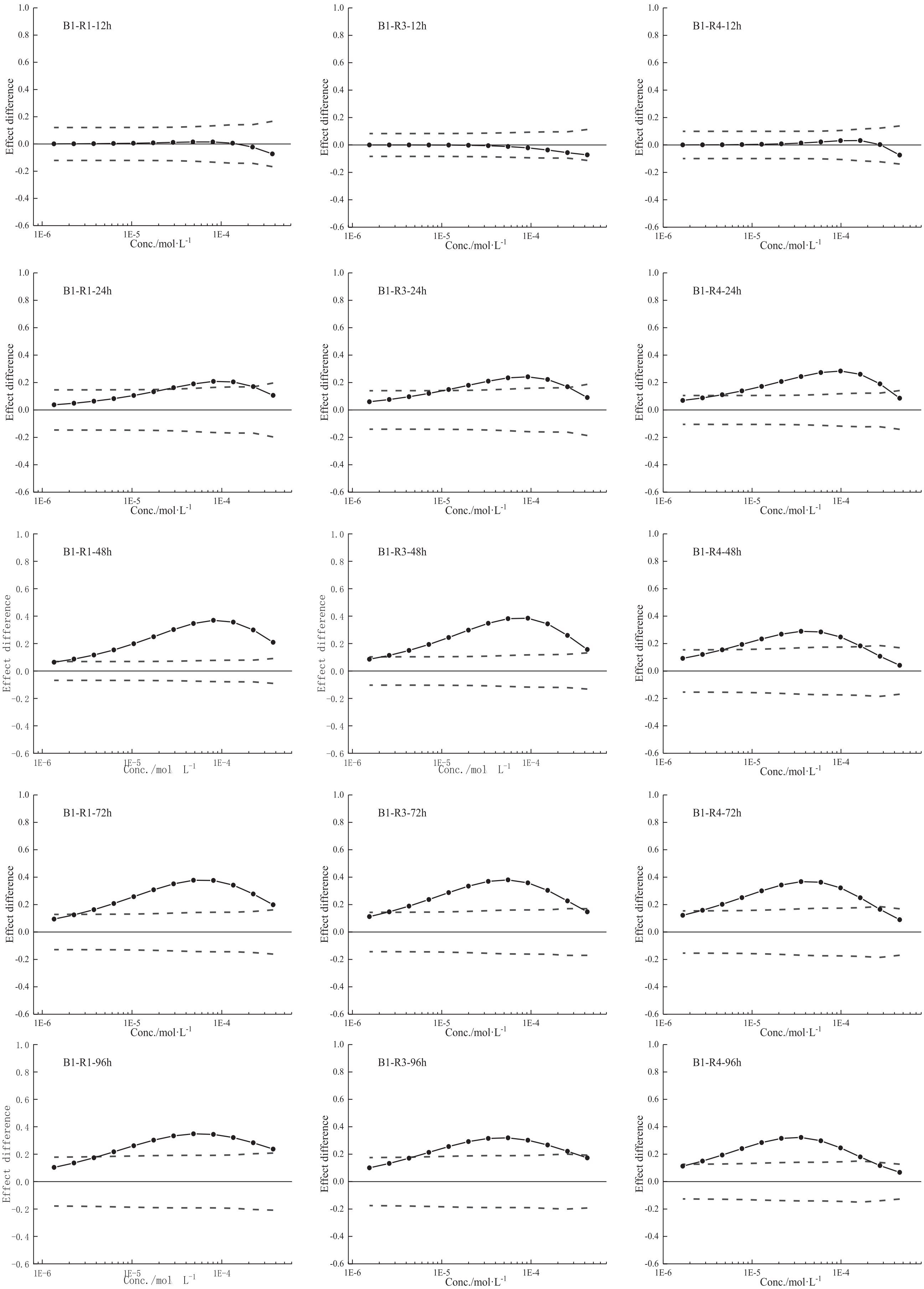

Fig. 1 Plot of RTZF curves of Zn-Cd binary mixture on *C pyrenoidosa* (- - -: 95% confidence interval; —: RTZF curve based on CA model).

the confidence interval in 72~96 h, and the combined toxicity appears additive action again. Overall, toxicity interaction within quinary heavy metal mixtures changes from additive action to antagonism and to additive action again over time.

The above results indicate that the type of toxicity interaction may vary with the concentration and exposure time of the quinary mixture system, even if the components are the same, which further confirmed the time-dependent and concentration-dependent

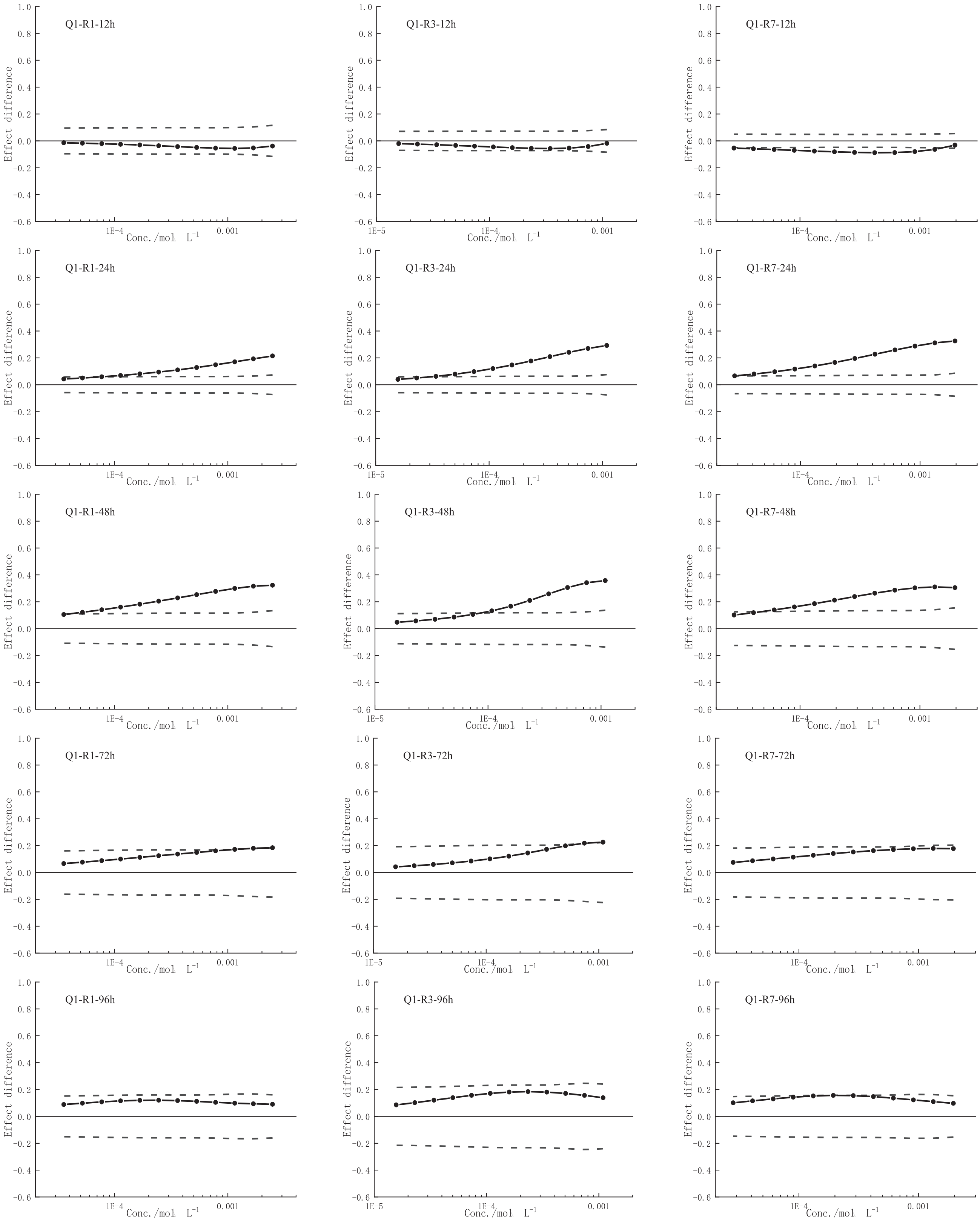

Fig. 2 Plot of RTZF curves of quinary mixture on *C pyrenoidosa*.

characteristics of the combined toxicity of heavy metal mixtures [36-37]. Yet, further studies on molecular level are needed to thoroughly understand the underlying mechanism of toxicity interaction, which will facilitate further investigations on the combined toxicity of multiple heavy metals.

Preliminary Study on the Toxicity Mechanism of Heavy Metals and Their Mixtures

Changes of Content of Chlorophyll-a in C. pyrenoidosa

Copper is an important component of electron transport associated with photosynthesis and respiration in phytoplankton [22]. Moreover, as the only binary mixture system with antagonism, it is necessary to preliminarily explore the mechanism of combined toxicity of Zn and Cd through more toxicity indicators. Therefore, heavy metals Cu, Zn, Cd and Zn-Cd binary mixture were selected for determination of chlorophyll-a content in this study. According to CRCs fitting parameters, the concentrations of the chemicals in each group were calculated when the inhibition effects on *C. pyrenoidosa* were 10%, 30%, 50% and 70%, respectively. The contents of chlorophyll-a in *C. pyrenoidosa* were determined in 48~96 h. Then, the chlorophyll-a reduction rate under different exposure time and inhibition effect was calculated. The results were presented in Fig. 3.

As illustrated in Fig. 3, the change of chlorophyll-a reduction rates is slightly different under the action of different contaminants. For the concentration with the growth inhibition of *C. pyrenoidosa* 10% exposed to Cu, the reduction rate of chlorophyll-a is close to 10%, while the reduction rate of chlorophyll-a is much higher than 10% when exposed to Zn and Cd. However, *C. pyrenoidosa* growth inhibition and chlorophyll-a reduction tend to be consistent when exposed to higher concentrations of heavy metals. Furthermore, the decrease rate of chlorophyll-a in Zn-Cd binary mixture is lower under different exposure concentrations. Taking 96 h exposure to Zn-Cd binary mixture as an example, when the inhibition effects are 10%, 30%, 50% and 70%, the reduction rates of chlorophyll-a are 7.75%, 24.88%, 41.30% and 57.69%, respectively.

At the lower exposure concentrations, the reduction rate of chlorophyll-a was significantly lower than that of Zn and Cd when exposed to Cu, which may be due to the fact that Cu is a trace element required by chloroplasts, and only exhibits obvious toxic effects at the higher concentrations [23, 26]. Interestingly, the reduction rate of chlorophyll-a in binary mixture was significantly lower than that of growth inhibition, and the reduction rate of chlorophyll-a was lower than that of single heavy metal exposure, thus it can be speculated that there are competition sites for toxic effects of heavy metals on the chloroplast.

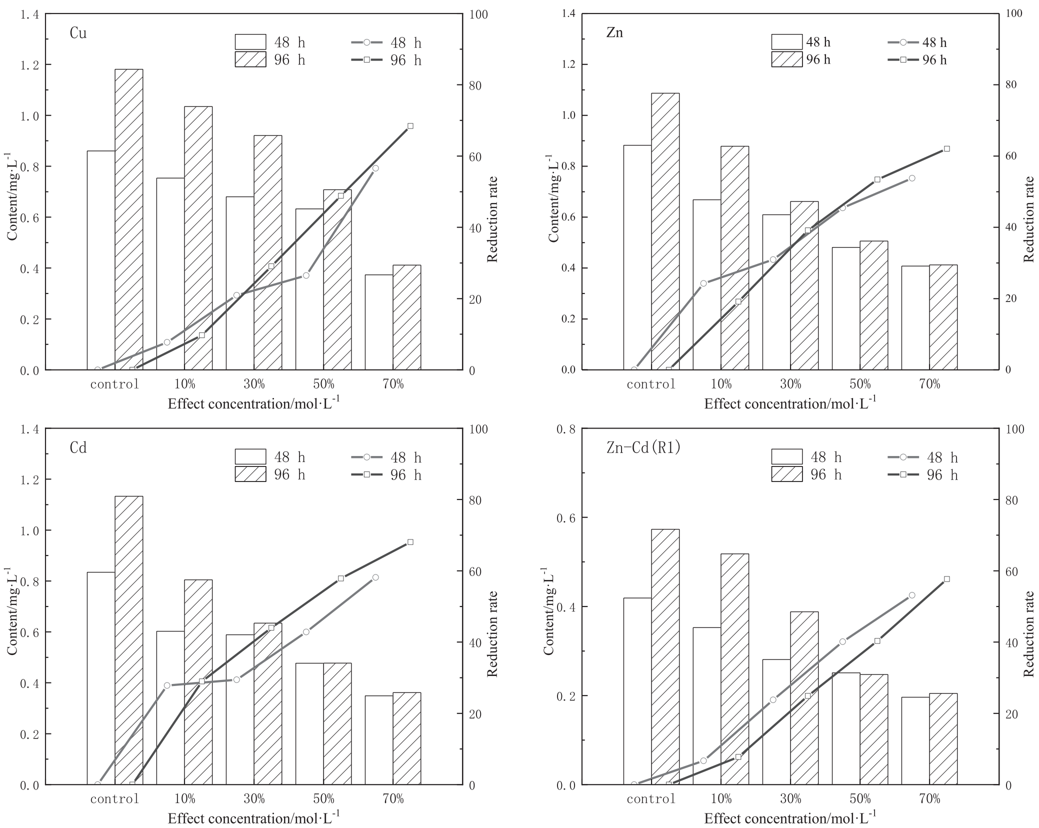

Fig. 3 Changes of chlorophyll-a content in *C pyrenoidosa* under different inhibition effect and exposure time.

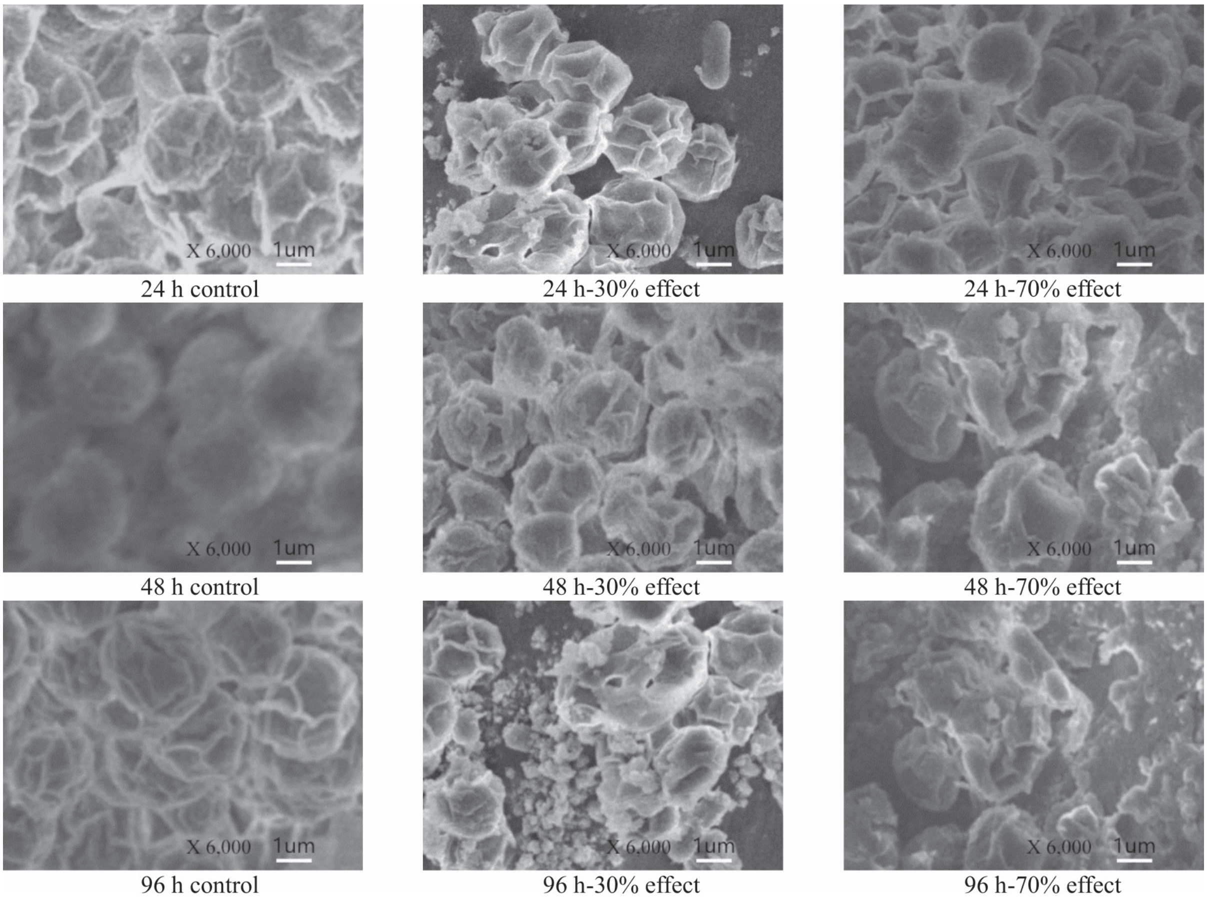

Fig. 4 Morphology of algal cells treated with copper at different effect concentration and exposure time.

SEM Images of Algal Cells

The same type of chemicals may have similar toxicity mechanisms to the test organisms. In addition, copper has the strongest toxic effect on *C. pyrenoidosa* among the five heavy metals, which makes it easier to observe obvious toxicity effect (Table S1).

The morphology of algal cells for different effect concentrations of copper in exposure time was observed by SEM (Fig. 4). As shown in Fig. 4, the algal cells in the blank group have complete structure and uniform folds on the surface, but the morphology of the algal cells changes significantly after copper sulfate treatment. With a growth inhibition effect of 30%, a small amount of content oozes out of the algal cells exposed for 24 h, the algal cells adhere to each other after 48 h, and the algal cells are seriously deformed after 96 h, with most of the cells even lyse. Under the concentration of 70% growth inhibition effect, the algal cells show irregular shapes and surface folds decrease exposed for 24 h, the algal cells ruptured and the contents of the cells flow out after 48 h, and the algal cells completely disintegrated after 96 h.

It is generally recognized that the toxicity mechanism of heavy metals to algae is that the activity of antioxidant enzymes in algal cells is reduced under the stress of heavy metals, and the active oxygen free genes produced in the body cannot be removed in time, which leads to membrane lipid peroxidation, thus destroying the membrane structure of algal cells [38]. However, some algal cell membranes were relatively intact exposed for 96 h under 30% inhibition effect, and almost all algal cell membranes were intact after 24 h under 70% inhibition effect. Therefore, it can be inferred that the toxicity mechanism of copper on algal cells not only destroys cell membrane structure, but also destroys chloroplast structure through cell membrane. In addition, some studies have found that copper can directly interact with the thylakoid membrane in the chloroplast, thereby adversely affecting the photosynthesis of algal cells [39-40], which is consistent with our hypothesis. Since the submicroscopic structure of algal cells has not been observed in this paper, the toxicity mechanism of heavy metal Cu on *C. pyrenoidosa* cannot be explored through changes in the internal structure of cells, which needs further study.

Conclusions

Concentration-effect data of 10 binary mixture systems and one quinary mixture on *C. pyrenoidosa* could be well fitted by Logit function. According to the RTZF method, nine binary mixture systems exhibited additive action and one mixture system (Zn-Cd) exhibited antagonism when the exposure time is longer than 24 h. Toxicity interaction of quinary heavy metal mixtures had obvious characteristics of time- and concentration-dependence. The growth inhibition of algal cells was not consistent with chlorophyll-a reduction rate under different heavy metals. The toxicity mechanism of copper on algal cells included destruction of cell membrane structure, and destruction of chloroplast structure through cell membrane.

Acknowledgements

The authors are especially grateful to the National Natural Science Foundation of China (No. 21677001), Natural Science Foundation of Anhui Province, China (No. 1708085MB50-1908085ME141) and Anhui Provincial Department of Education College Natural Science Research Project (No.KJ2019A0757, KJ2015JD06) for their financial support.

Conflict of Interest

The authors declare no conflict of interest.

References

1. SINGH H., PANDEY R., SINGH S.K., SHUKLA D.N. Assessment of heavy metal contamination in the sediment of the River Ghaghara, a major tributary of the River Ganga in Northern India. Appl. Water. Sci. **7**, 4133, **2017**.
2. DAO T.S., LE V.N., BUI B.T., DINH K.V., WIEGAND C., NGUYEN T.S., DAO C.T., NGUYEN V.D., TO T.H., NGUYEN L.S.P., VO T.G., VO T.M.C. Sensitivity of a tropical micro-crustacean (Daphnia lumholtzi) to trace metals tested in natural water of the Mekong River. Sci. Total Environ. **574**, 1360, **2016**.
3. ZHONG Z., WANG H.Y., KONG X.Q., YANG Y.Y., LI L., HANG Q.Y. Distribution characteristics, sources identification and risk assessment of heavy metals in surface sediments of urban rivers in Kaifeng. Acta Scien. Circum. **36**, 4520, **2016** [In Chinese].
4. LIU Z.Q., XU F.J., TIAN X., ZHAO Y.F., LI A.C., JIANG Z.Z., YIN X.B. Evaluation of heavy metals pollution in surface sediments of the intertidal Jiaozhou Bay, China. China Environ. Sci. **37**, 2239, **2017** [In Chinese].
5. GONG Y., ZHAO D., WANG Q. An overview of field-scale studies on remediation of soil contaminated with heavy metals and metalloids: Technical progress over the last decade. Water Res. **147**, 440, **2018**.
6. DERAKHSHAN N.Z., JUNG M.C., KIM K.H. Remediation of soils contaminated with heavy metals with an emphasis on immobilization technology. Environ. Geochem. Health. **40**, 927, **2018**.
7. DU C.L., WU J.H., BASHIR M.H., SHAUKAT M., ALI S. Heavy metals transported through a multi-trophic food chain influence the energy metabolism and immune responses of *Cryptolaemus montrouzieri*. Ecotoxicology. **28**, 422, **2019**.
8. ZHANG J., LIU S.S., DONG X.Q., CHEN M. Predictability of the time-dependent toxicities of aminoglycoside antibiotic mixtures to *Vibrio qinghaiensis* sp. -Q67. Rsc Adv. **5**, 107076, **2015**.
9. YORIFUJI T., TSUDA T. Epidemiological studies of neurological signs and symptoms and blood pressure in populations near the industrial methylmercury contamination at Minamata, Japan. Arch. Environ. Occup. Health. **71**, 231, **2016**.
10. KOBAYASHI E., SUWAZONO Y., DOCHI M., HONDA R., KIDO T. Influence of consumption of cadmium-polluted rice or Jinzu River Water on occurrence of renal tubular dysfunction and/or itai-itai disease. Biol. Trace Elem. Res. **127**, 257, **2009**.
11. ZHANG J., LIU S.S., XIAO Q.F., HUANG X.H., CHEN Q. Identifying the component responsible for antagonism within ionic liquid mixtures using the up-to-down procedure integrated with a uniform design ray method. Ecotoxicol. Environ. Saf. **107**, 16, **2014**.
12. FAUST M., ALTENBURGER R., BACKHAUS T., BLANCK H., BOEDEKER W., GRAMATICA P., HAMER V., SCHOLZE M., VIGHI M., GRIMME L.H. Predicting the joint algal toxicity of multi-component s-triazine mixtures at low-effect concentrations of individual toxicants. Aquat. Toxicol. **56**, 13, **2001**.
13. WOLLENBERGER L., HALLING-SØRENSEN B., KUSK K.O. Acute and chronic toxicity of veterinary antibiotics to *Daphnia magna*. Chemosphere. **40**, 723, **2000**.
14. QU R., LIU S.S., CHEN F., LI K. Complex toxicological interaction between ionic liquid and pesticide to *Vibrio qinghaiensis* sp.-Q67. Rsc Adv. **6**, 21012, **2016**.
15. LIU S.S. Assessment and prediction of toxicity of chemical mixtures, first ed. Science Press, Bei Jing, China, pp. 100-118, **2017** [In Chinese].
16. CHEN Q., ZHANG J., LI X.M., LIU L. Time-dependent microplate toxicity analysis (T-MTA) of several antibiotics to *Chlorella pyrenoidosa*. Asian J. Ecotoxicol. **10**, 190, **2015** [In Chinese].
17. DOU R.N., LIU S.S., MO L.Y., LIU H.L., DENG C F. A novel direct equipartition ray design (EquRay) procedure for toxicity interaction between ionic liquid and dichlorvos. Environ. Sci. Pollut. Res. Int. **18**, 734, **2011**.
18. LIU S.S., XIAO Q.F., ZHANG J., YU M. Uniform design ray in the assessment of combined toxicities of multi-component mixtures. Chin. Sci. Bull. **61**, 52, **2016**.
19. BACKHAUS T., ARRHENIUS A., BLANCK H. Toxicity of a mixture of dissimilarly acting substances to natural algal communities: predictive power and limitations of independent action and concentration addition. Environ. Sci. Technol. **38**, 6363, **2005**.
20. HUANG W.Y., LIU F., LIU S.S., GE H.L., CHEN, H.H. Predicting mixture toxicity of seven phenolic compounds with similar and dissimilar action mechanisms to *Vibrio qinghaiensis* sp.nov.Q67. Ecotoxicol. Environ. Saf. **74**, 1600, **2011**.
21. ZHANG J., LIU S.S., DOU R.N., LIU H.L., ZHANG J. Evaluation on the toxicity of ionic liquid mixture with antagonism and synergism to *Vibrio qinghaiensis* sp.-Q67. Chemosphere. **82**, 1024, **2011**.
22. OUYANG H.L., KONG X.Z., QIN N., HE W., HE Q.S., WANG Y., WANG R., XU F.L. Effects of five heavy metals at sub-lethal concentrations on the growth and photosynthesis of *Chlorella vulgaris*. Chin Sci Bull. **57**, 785, **2012**.

23. KONDZIOR P., BUTAREWICZ A. Effect of heavy metals (Cu and Zn) on the content of photosynthetic pigments in the cells of Algae *Chlorella vulgaris*. J. Ecol. Eng. **19**, 18, **2012**.
24. FAN H.Y., JIN M.K., WANG H., XU Q.R., XU L., WANG C.X.Z., DU S.T., LIU H.J. Effect of differently methyl-substituted ionic liquids on *Scenedesmus obliquus* growth, photosynthesis, respiration, and ultrastructure. Environ Pollut. **250**, 155, **2019**.
25. GEOFFROY L., DEWEZ D., VERNET G., POPOVIC R. Different physiological parameters used in evaluation of oxyfluorfen effect on S.obliquus: validity of parameters as biomarkers, Arch. Environ. Con. Tox. **45**, 439, **2003**.
26. ECHEVESTE P., SILVA J.C., LOMBARDI A.T. Cu and Cd affect distinctly the physiology of a cosmopolitan tropical freshwater phytoplankton. Ecotoxicol. Environ. Saf. **143**, 228, **2017**.
27. LI W., YUN Y., SHI Y.Y., ZHANG Y.L. Effects of 5-fluorouracil on the growth and chlorophyll content of *Chlorella pyrenoidosa* and *Selenastrum capricornutum*. Asian J. Ecotoxicol. **10**, 213, **2015** [In Chinese].
28. LIU H., XIA Y., FAN H., XU Q., DU S., FANG Z.G., XIA H.L. Effect of imidazolium-based ionic liquids with varying carbon chain lengths on *Arabidopsis thaliana*: Response of growth and photosynthetic fluorescence parameters. J. Hazard. Mater. **358**, 327, **2018**.
29. YU P.F., LIU H., MOU Z.J., LU Z.X., LI S.H., ZHANG D.H., HE H.Z. Acute toxic effects of silver nanoparticles and silver ion on two microalgae. Asian J. Ecotoxicol. **12**, 188, **2017** [In Chinese].
30. MARTINEZ-RUIZ E.B., MARTINEZ-JERONIMO F. Exposure to the herbicide 2,4-D produces different toxic effects in two different phytoplankters: A green microalga (*Ankistrodesmus falcatus*) and a toxigenic cyanobacterium (*Microcystis aeruginosa*). Sci Total Environ. **619**, 1566, **2018**.
31. MEYER J.S., FARLEY K.J., GARMAN E.R. Metal mixtures modeling evaluation project: 1. Background. Environ. Toxicol. Chem. **34**, 726, **2015**.
32. GROTEN J.P., FERON V.J., SÜHNEL J. Toxicology of simple and complex mixtures. Trends Pharmacol. Sci. **22**, 316, **2001**.
33. DING Z., LIU J., GAO J., MUHAMMAD, S., HAN, Z.Q., WANG Z., LI J.K., SJOLINDER H. Zinc supplementation protects against cadmium accumulation and cytotoxicity in madin-darby bovine kidney cells. Plos One. **9**, 103427, **2014**.
34. STERENBORG I., VORK N.A., VERKADE S.K., GESTEL C.A.M.V., STRAALEN N.M.V. Dietary zinc reduces uptake but not metallothionein binding and elimination of cadmium in the springtail, Orchesella cincta. Environ. Toxicol. Chem. **22**, 1167, **2003**.
35. PEREZ E., HOANG T.C. Chronic toxicity of binary-metal mixtures of cadmium and zinc to Daphnia magna. Environ. Toxicol. Chem. **36**, 2739, **2017**.
36. ZHANG J., DING T.T., DONG X.Q., BIAN Z.Q. Time-dependent and Pb-dependent antagonism and synergism towards *Vibrio qinghaiensis* sp.-Q67 within heavy metal mixtures. Rsc Adv. **8**, 26089, **2018**.
37. FENG L., LIU S.S., LI K., TANG H.X., LIU H.L. The time-dependent synergism of the six-component mixtures of substituted phenols, pesticides and ionic liquids to *Caenorhabditis elegans*. J. Hazard. Mater. **327**, 11, **2017**.
38. TUKAJ Z., POKORA W. Individual and combined effect of anthracene, cadmium, and chloridazone on growth and activity of SOD izoformes in three *Scenedesmus* species. Ecotoxicol. Environ. Saf. **65**, 323, **2006**.
39. ZHOU S., SHAO Y., GAO N., DENG Y., QIAO J., OU H.S., DENG J. Effects of different algaecides on the photosynthetic capacity, cell integrity and microcystin-LR release of *Microcystis aeruginosa*. Sci. Total Environ. **463-464**, 111, **2013**.
40. ZHANG H., MENG G., MAO F., LI W., HE Y., GIN K.Y.H., ONG C.N. Use of an integrated metabolomics platform for mechanistic investigations of three commonly used algaecides on *cyanobacterium*, *Microcystis aeruginosa*. J. Hazard. Mater. **367**, 120, **2019**.

Supplementary Materials

Table S1. The Logit function fitting parameters and statistics, mean effect concentration and its negative logarithm for the five heavy metals.

Name	Time/h	Parameters				EC_{50} (mol/L)	pEC_{50}
		α	β	RMSE	R		
Cu	12	10.81	3.23	0.057	0.8240	∞	0
	24	10.69	2.84	0.0745	0.9442	∞	0
	48	15.00	3.54	0.076	0.9790	5.79E-05	4.24
	72	15.00	3.53	0.085	0.9860	5.63E-05	4.25
	96	15.00	3.52	0.090	0.9800	5.48E-05	4.26
Mn	12	0.01	6.00	0.162	–0.121	∞	0
	24	1.45	1.00	0.045	0.9130	∞	0
	48	3.09	1.12	0.036	0.9800	1.74E-03	2.76
	72	3.96	1.34	0.070	0.9490	1.11E-03	2.96
	96	4.04	1.3	0.124	0.8900	7.80E-04	3.11
Cd	12	8.82	3.62	0.063	0.9640	∞	0
	24	3.51	1.17	0.078	0.9200	1.00E-03	3.00
	48	5.20	1.44	0.083	0.9480	2.45E-04	3.61
	72	5.56	1.46	0.073	0.9600	1.56E-04	3.81
	96	6.89	1.77	0.055	0.9810	1.28E-04	3.89
Zn	12	5.93	2.47	0.049	0.9170	∞	0
	24	5.03	1.75	0.035	0.9810	1.34E-03	2.87
	48	5.22	1.56	0.031	0.9900	4.51E-04	3.35
	72	5.46	1.50	0.041	0.9860	2.29E-04	3.64
	96	6.00	1.52	0.054	0.9780	1.13E-04	3.95
Pb	12	3.33	2.52	0.025	0.6140	∞	0
	24	4.8	1.61	0.028	0.9900	1.04E-03	2.98
	48	11.22	3.47	0.064	0.9860	5.84E-04	3.23
	72	15.00	4.74	0.096	0.9810	6.85E-04	3.16
	96	15.00	4.81	0.106	0.9770	7.61E-04	3.12

Table S2. The Logit function fitting parameters and statistics, mean effect concentration and its negative logarithm for the Zn-Mn binary mixture.

Ray	Time/h	Parameters				EC_{50} (mol/L)	pEC_{50}
		α	β	RMSE	R		
R1	12	3.18	1.24	0.097	0.8553	2.73E-03	2.56
	24	4.33	1.4	0.066	0.9538	8.08E-04	3.09
	48	5.43	1.52	0.041	0.9851	2.68E-04	3.57
	72	5.42	1.42	0.057	0.9726	1.52E-04	3.82
	96	6.08	1.56	0.062	0.9727	1.27E-04	3.90

Table S2. Continued.

R2	12	0.58	0.47	0.073	0.6716	5.83E-02	1.23
	24	2.45	0.87	0.049	0.9464	1.53E-03	2.82
	48	4.21	1.21	0.042	0.9792	3.32E-04	3.48
	72	4.17	1.09	0.055	0.9615	1.49E-04	3.83
	96	4.49	1.14	0.063	0.9531	1.15E-04	3.94
R3	12	1.86	1.04	0.063	0.8532	1.63E-02	1.79
	24	1.73	0.79	0.064	0.8781	6.46E-03	2.19
	48	3.7	1.15	0.035	0.9845	6.06E-04	3.22
	72	4.27	1.24	0.074	0.9441	3.60E-04	3.44
	96	4.7	1.37	0.102	0.9139	3.71E-04	3.43
R4	12	0.01	0.65	0.087	0.0880	9.65E-01	0.02
	24	1.09	0.66	0.057	0.8611	2.23E-02	1.65
	48	3.99	1.3	0.043	0.9800	8.53E-04	3.07
	72	4.68	1.41	0.085	0.9366	4.80E-04	3.32
	96	5.29	1.6	0.114	0.9096	4.94E-04	3.31
R5	12	0.16	0.73	0.078	0.5593	6.04E-01	0.22
	24	1.54	0.81	0.062	0.8802	1.26E-02	1.90
	48	3.64	1.19	0.043	0.9771	8.73E-04	3.06
	72	4.92	1.49	0.073	0.9553	4.99E-04	3.30
	96	6.37	1.98	0.090	0.9538	6.06E-04	3.22

Table S3. The Logit function fitting parameters and statistics, mean effect concentration and its negative logarithm for the Zn-Pb binary mixture.

Ray	Time/h	Parameters				EC_{50}	pEC_{50}
		α	β	RMSE	R		
R1	12	0.28	0.47	0.043	0.7510	2.54E-01	0.60
	24	2.32	0.87	0.039	0.9470	2.15E-03	2.67
	48	4.30	1.32	0.094	0.8810	5.53E-04	3.26
	72	14.71	4.48	0.124	0.9270	5.21E-04	3.28
	96	15.00	4.60	0.092	0.9600	5.48E-04	3.26
R2	12	1.70	0.90	0.060	0.8090	1.29E-02	1.89
	24	3.81	1.32	0.044	0.9660	1.30E-03	2.89
	48	8.25	2.46	0.057	0.9790	4.43E-04	3.35
	72	15.00	4.48	0.082	0.9810	4.49E-04	3.35
	96	15.00	4.56	0.064	0.9840	5.13E-04	3.29
R3	12	1.73	0.92	0.041	0.9050	1.32E-02	1.88
	24	3.57	1.23	0.038	0.9750	1.25E-03	2.90
	48	7.53	2.26	0.060	0.9750	4.66E-04	3.33
	72	15.00	4.56	0.095	0.9650	5.13E-04	3.29
	96	15.00	4.62	0.072	0.9770	5.67E-04	3.25

Table S3. Continued.

R4	12	1.62	0.87	0.037	0.9210	1.37E-02	1.86
	24	3.39	1.13	0.045	0.9660	1.00E-03	3.00
	48	8.84	2.60	0.083	0.9620	3.98E-04	3.40
	72	15.00	4.45	0.122	0.9610	4.26E-04	3.37
	96	15.00	4.49	0.112	0.9610	4.56E-04	3.34
R5	12	2.01	0.92	0.055	0.8880	6.53E-03	2.19
	24	3.95	1.29	0.052	0.9630	8.67E-04	3.06
	48	9.06	2.66	0.079	0.9670	3.93E-04	3.41
	72	15.00	4.49	0.130	0.9550	4.56E-04	3.34
	96	15.00	4.51	0.117	0.9560	4.72E-04	3.33

Table S4. The Logit function fitting parameters and statistics, mean effect concentration and its negative logarithm for the Zn-Cd binary mixture.

Ray	Time/h	Parameters				EC_{50}	pEC_{50}
		α	β	RMSE	R		
R1	12	11.28	3.44	0.050	0.9150	5.26E-04	3.28
	24	9.78	2.9	0.060	0.9183	4.24E-04	3.37
	48	10.23	2.95	0.028	0.9860	3.41E-04	3.47
	72	8.93	2.48	0.053	0.9643	2.51E-04	3.60
	96	6.37	1.70	0.072	0.9378	1.79E-04	3.75
R2	12	14.99	4.61	0.076	0.9118	5.60E-04	3.25
	24	12.22	3.63	0.070	0.9107	4.30E-04	3.37
	48	9.32	2.68	0.034	0.9875	3.33E-04	3.48
	72	8.28	2.26	0.046	0.9803	2.17E-04	3.66
	96	7.94	2.05	0.050	0.9794	1.34E-04	3.87
R3	12	9.28	2.88	0.034	0.9718	5.99E-04	3.22
	24	9.64	2.86	0.058	0.9450	4.26E-04	3.37
	48	10.66	3.02	0.042	0.9809	2.95E-04	3.53
	72	9.25	2.52	0.059	0.9676	2.13E-04	3.67
	96	7.15	1.85	0.071	0.9555	1.37E-04	3.86
R4	12	15	4.60	0.041	0.9473	5.48E-04	3.26
	24	10.95	3.26	0.043	0.9653	4.38E-04	3.36
	48	9.79	2.76	0.040	0.9894	2.84E-04	3.55
	72	9.91	2.64	0.063	0.9844	1.76E-04	3.75
	96	9.69	2.43	0.052	0.9893	1.03E-04	3.99
R5	12	2.18	0.85	0.069	0.7790	2.72E-03	2.56
	24	4.27	1.33	0.042	0.9554	6.16E-04	3.21
	48	5.63	1.58	0.043	0.9749	2.73E-04	3.56
	72	6.58	1.68	0.045	0.9841	1.21E-04	3.92
	96	6.9	1.63	0.030	0.9934	5.85E-05	4.23

Table S5. The Logit function fitting parameters and statistics, mean effect concentration and its negative logarithm for the Zn-Cu binary mixture.

Ray	Time/h	Parameters				EC_{50}	pEC_{50}
		α	β	RMSE	R		
R1	12	6.98	2.02	0.061	0.8924	3.50E-04	3.46
	24	7.49	2.02	0.065	0.9393	1.96E-04	3.71
	48	11.07	2.79	0.028	0.9909	1.08E-04	3.97
	72	15	3.71	0.059	0.9705	9.05E-05	4.04
	96	10.84	2.58	0.073	0.9609	6.29E-05	4.20
R2	12	0.01	0.31	0.083	0.2862	9.28E-01	0.03
	24	3.12	0.93	0.071	0.7855	4.42E-04	3.35
	48	9.6	2.34	0.044	0.9725	7.90E-05	4.10
	72	14.05	3.27	0.073	0.9640	5.05E-05	4.30
	96	13.95	3.15	0.064	0.9755	3.73E-05	4.43
R3	12	8.22	2.15	0.063	0.8400	1.50E-04	3.82
	24	5.41	1.53	0.044	0.8796	2.91E-04	3.54
	48	11.86	2.89	0.056	0.9416	7.87E-05	4.10
	72	14.98	3.45	0.093	0.9342	4.55E-05	4.34
	96	15	3.32	0.068	0.9703	3.03E-05	4.52
R4	12	0.01	0.51	0.054	0.2733	9.56E-01	0.02
	24	3.02	0.99	0.039	0.8513	8.90E-04	3.05
	48	10.22	2.42	0.042	0.9692	5.98E-05	4.22
	72	14.74	3.24	0.123	0.9559	2.82E-05	4.55
	96	14.99	3.16	0.124	0.9756	1.80E-05	4.74
R5	12	15	3.71	0.129	0.6755	9.05E-05	4.04
	24	15	3.54	0.078	0.9036	5.79E-05	4.24
	48	15	3.32	0.074	0.9916	3.03E-05	4.52
	72	15	3.18	0.092	0.9683	1.92E-05	4.72
	96	15	3.10	0.089	0.9684	1.45E-05	4.84

Table S6. The Logit function fitting parameters and statistics, mean effect concentration and its negative logarithm for the Mn-Cu binary mixture.

Ray	Time/h	Parameters				EC_{50}	pEC_{50}
		α	β	RMSE	R		
R1	12	1.55	1.08	0.033	0.9406	3.67E-02	1.44
	24	1.67	1.07	0.050	0.9128	2.75E-02	1.56
	48	3.24	1.31	0.068	0.9458	3.36E-03	2.47
	72	3.9	1.10	0.057	0.9595	2.85E-04	3.55
	96	4.97	1.40	0.082	0.9435	2.82E-04	3.55

Table S6. Continued.

R2	12	0.01	0.39	0.078	0.2782	9.43E-01	0.03
	24	0.66	0.69	0.037	0.8929	1.11E-01	0.96
	48	3.5	1.43	0.087	0.9223	3.57E-03	2.45
	72	6.25	1.89	0.086	0.9639	4.93E-04	3.31
	96	7.16	2.16	0.058	0.9850	4.84E-04	3.31
R3	12	0.01	0.87	0.084	-0.3657	9.74E-01	0.01
	24	0.01	0.62	0.048	0.5419	9.64E-01	0.02
	48	1.56	0.83	0.042	0.9314	1.32E-02	1.88
	72	3.51	1.00	0.052	0.9603	3.09E-04	3.51
	96	4.67	1.35	0.047	0.9794	3.47E-04	3.46
R4	12	0.01	0.69	0.093	-0.1068	9.67E-01	0.01
	24	0.08	0.65	0.049	0.6874	7.53E-01	0.12
	48	2.05	0.99	0.075	0.8572	8.50E-03	2.07
	72	4.12	1.17	0.060	0.9602	3.01E-04	3.52
	96	5.3	1.50	0.051	0.9800	2.93E-04	3.53
R5	12	0.8	0.98	0.080	0.4591	1.53E-01	0.82
	24	0.86	0.89	0.073	0.5544	1.08E-01	0.97
	48	2.07	0.91	0.049	0.9176	5.31E-03	2.27
	72	3.64	0.91	0.086	0.8830	1.00E-04	4.00
	96	4.45	1.15	0.051	0.9696	1.35E-04	3.87

Table S7. The Logit function fitting parameters and statistics, mean effect concentration and its negative logarithm for the Pb-Cu binary mixture.

Ray	Time/h	Parameters				EC_{50}	pEC_{50}
		α	β	RMSE	R		
R1	12	0.01	1.12	0.090	0.2759	9.80E-01	0.01
	24	4.1	1.76	0.069	0.8659	4.68E-03	2.33
	48	3.64	1.29	0.086	0.8915	1.51E-03	2.82
	72	4.33	1.30	0.102	0.8978	4.67E-04	3.33
	96	5.38	1.45	0.108	0.9128	1.95E-04	3.71
R2	12	0.79	0.93	0.075	0.5214	1.41E-01	0.85
	24	3.57	1.43	0.045	0.9394	3.19E-03	2.$_{50}$
	48	5.04	1.64	0.100	0.9183	8.45E-04	3.07
	72	6.54	1.85	0.124	0.9253	2.92E-04	3.54
	96	7.8	2.02	0.101	0.9545	1.38E-04	3.86
R3	12	0.08	0.77	0.048	0.5915	7.87E-01	0.10
	24	2.46	1.04	0.056	0.8927	4.31E-03	2.37
	48	3.63	1.14	0.096	0.8788	6.54E-04	3.18
	72	5.23	1.39	0.119	0.8919	1.73E-04	3.76
	96	6.39	1.54	0.090	0.9419	7.09E-05	4.15

Table S7. Continued.

R4	12	0.03	0.61	0.048	0.6010	8.93E-01	0.05
	24	3.16	1.14	0.066	0.8822	1.69E-03	2.77
	48	5.08	1.42	0.106	0.9047	2.65E-04	3.58
	72	6.84	1.68	0.131	0.9071	8.48E-05	4.07
	96	10.06	2.30	0.123	0.9446	4.23E-05	4.37
R5	12	1.22	0.92	0.055	0.6111	4.72E-02	1.33
	24	2.86	0.94	0.076	0.8360	9.07E-04	3.04
	48	4.98	1.23	0.103	0.8940	8.94E-05	4.05
	72	7.2	1.55	0.122	0.9027	2.26E-05	4.65
	96	10.06	2.04	0.123	0.9233	1.17E-05	4.93

Table S8. The Logit function fitting parameters and statistics, mean effect concentration and its negative logarithm for the Cd-Cu binary mixture.

Ray	Time/h	Parameters				EC_{50}	pEC_{50}
		α	β	RMSE	R		
R1	12	2.86	0.98	0.033	0.9446	1.21E-03	2.92
	24	4.12	1.09	0.080	0.9000	1.66E-04	3.78
	48	5.25	1.27	0.127	0.8630	7.35E-05	4.13
	72	6.86	1.55	0.129	0.8994	3.75E-05	4.43
	96	8.83	1.92	0.107	0.9479	2.52E-05	4.60
R2	12	0.98	0.70	0.052	0.5115	3.98E-02	1.40
	24	2.91	0.85	0.054	0.9001	3.77E-04	3.42
	48	5.29	1.28	0.074	0.9344	7.37E-05	4.13
	72	8.12	1.80	0.132	0.9161	3.08E-05	4.51
	96	9.89	2.08	0.118	0.9462	1.76E-05	4.75
R3	12	3.21	1.06	0.045	0.8363	9.37E-04	3.03
	24	3.46	0.90	0.052	0.9218	1.43E-04	3.84
	48	5.21	1.21	0.032	0.9835	4.95E-05	4.31
	72	6.63	1.38	0.052	0.9750	1.57E-05	4.80
	96	8.18	1.67	0.045	0.9860	1.26E-05	4.90
R4	12	0.01	0.47	0.058	0.2249	9.52E-01	0.02
	24	2.76	0.75	0.064	0.8480	2.09E-04	3.68
	48	5.88	1.27	0.087	0.9157	2.34E-05	4.63
	72	7.92	1.59	0.133	0.8995	1.04E-05	4.98
	96	9.37	1.81	0.108	0.9432	6.66E-06	5.18
R5	12	1.98	0.86	0.027	0.8236	4.99E-03	2.30
	24	3.83	0.96	0.042	0.9422	1.02E-04	3.99
	48	5.6	1.21	0.043	0.9712	2.35E-05	4.63
	72	7.48	1.45	0.089	0.9406	6.94E-06	5.16
	96	9.03	1.69	0.088	0.9562	4.54E-06	5.34

Table S9. The Logit function fitting parameters and statistics, mean effect concentration and its negative logarithm for the Mn-Cu binary mixture.

Ray	Time/h	Parameters				EC_{50}	pEC_{50}
		α	β	RMSE	R		
R1	12	0.22	0.79	0.064	0.5455	5.27E-01	0.28
	24	1.23	0.84	0.062	0.8217	3.43E-02	1.46
	48	3.82	1.53	0.045	0.9743	3.19E-03	2.50
	72	4.65	1.64	0.042	0.9833	1.46E-03	2.84
	96	5.47	1.8	0.040	0.9880	9.14E-04	3.04
R2	12	0.01	0.69	0.086	0.2640	9.67E-01	0.01
	24	1.67	0.84	0.065	0.8443	1.03E-02	1.99
	48	4.02	1.43	0.048	0.9707	1.54E-03	2.81
	72	5.75	1.79	0.070	0.9704	6.13E-04	3.21
	96	7.36	2.12	0.059	0.9842	3.38E-04	3.47
R3	12	2.06	1.04	0.051	0.8487	1.05E-02	1.98
	24	2.98	1.10	0.044	0.9550	1.95E-03	2.71
	48	3.52	1.17	0.049	0.9618	9.81E-04	3.01
	72	5.34	1.52	0.086	0.9483	3.07E-04	3.51
	96	6.16	1.63	0.076	0.9640	1.66E-04	3.78
R4	12	2.46	1.14	0.048	0.8327	6.95E-03	2.16
	24	3.16	1.11	0.046	0.9449	1.42E-03	2.85
	48	3.94	1.23	0.051	0.9591	6.26E-04	3.20
	72	6.24	1.66	0.094	0.9466	1.74E-04	3.76
	96	6.96	1.73	0.090	0.9557	9.48E-05	4.02
R5	12	2.9	1.25	0.041	0.8232	4.79E-03	2.32
	24	3.42	1.06	0.054	0.9332	5.94E-04	3.23
	48	5.28	1.45	0.059	0.9593	2.28E-04	3.64
	72	6.97	1.70	0.089	0.9519	7.94E-05	4.10
	96	8.68	2.03	0.086	0.9680	5.30E-05	4.28

Table S10. The Logit function fitting parameters and statistics, mean effect concentration and its negative logarithm for the Pb-Cd binary mixture.

Ray	Time/h	Parameters				EC_{50}	pEC_{50}
		α	β	RMSE	R		
R1	12	1.79	1.06	0.075	0.7647	2.05E-02	1.69
	24	2.31	1.01	0.080	0.8353	5.16E-03	2.29
	48	3.66	1.23	0.101	0.8815	1.06E-03	2.98
	72	5.13	1.52	0.141	0.8732	4.22E-04	3.38
	96	5.23	1.46	0.116	0.9047	2.62E-04	3.58

Table S10. Continued.

R2	12	0.64	0.73	0.066	0.6594	1.33E-01	0.88
	24	1.43	0.77	0.070	0.7880	1.39E-02	1.86
	48	3.72	1.27	0.092	0.8964	1.18E-03	2.93
	72	5.04	1.51	0.111	0.9090	4.59E-04	3.34
	96	5.93	1.69	0.104	0.9328	3.10E-04	3.51
R3	12	1.06	0.79	0.087	0.6441	4.55E-02	1.34
	24	1.97	0.89	0.092	0.7648	6.12E-03	2.21
	48	3.38	1.14	0.085	0.8947	1.08E-03	2.96
	72	4.42	1.32	0.101	0.9049	4.48E-04	3.35
	96	5.25	1.47	0.118	0.9016	2.68E-04	3.57
R4	12	0.01	0.43	0.072	0.5022	9.48E-01	0.02
	24	1.22	0.65	0.081	0.7022	1.33E-02	1.88
	48	3.64	1.21	0.072	0.9242	9.81E-04	3.01
	72	4.86	1.43	0.100	0.9176	3.99E-04	3.40
	96	7.27	2.06	0.095	0.9585	2.96E-04	3.53
R5	12	1.46	0.86	0.055	0.8118	2.01E-02	1.70
	24	2.52	0.99	0.050	0.9249	2.85E-03	2.55
	48	4.27	1.32	0.053	0.9674	5.82E-04	3.23
	72	5.30	1.51	0.102	0.9201	3.09E-04	3.51
	96	6.96	1.91	0.090	0.9570	2.27E-04	3.64

Table S11. The Logit function fitting parameters and statistics, mean effect concentration and its negative logarithm for the Pb-Mn binary mixture.

Ray	Time/h	Parameters				EC_{50}	pEC_{50}
		α	β	RMSE	R		
R1	12	1.01	0.79	0.077	0.6841	5.27E-02	1.28
	24	2.74	1.16	0.076	0.8705	4.34E-03	2.36
	48	4.10	1.41	0.087	0.9180	1.24E-03	2.91
	72	5.36	1.64	0.096	0.9357	5.39E-04	3.27
	96	6.04	1.76	0.092	0.9489	3.70E-04	3.43
R2	12	0.01	0.44	0.060	0.4049	9.49E-01	0.02
	24	1.79	0.85	0.079	0.8138	7.84E-03	2.11
	48	3.75	1.31	0.100	0.8944	1.37E-03	2.86
	72	5.54	1.70	0.119	0.9196	5.51E-04	3.26
	96	6.70	1.96	0.118	0.9372	3.82E-04	3.42
R3	12	0.50	0.70	0.059	0.7140	1.93E-01	0.71
	24	2.13	1.05	0.060	0.8908	9.36E-03	2.03
	48	3.39	1.26	0.078	0.9206	2.04E-03	2.69
	72	4.42	1.39	0.099	0.9199	6.61E-04	3.18
	96	5.10	1.47	0.083	0.9493	3.39E-04	3.47

Table S11. Continued.

R4	12	0.01	0.58	0.063	0.3868	9.61E-01	0.02
	24	1.31	0.86	0.070	0.8099	3.00E-02	1.52
	48	3.00	1.21	0.104	0.8675	3.32E-03	2.48
	72	3.77	1.25	0.118	0.8777	9.64E-04	3.02
	96	4.57	1.35	0.097	0.9231	4.12E-04	3.39
R5	12	0.01	0.58	0.126	0.0907	9.61E-01	0.02
	24	0.48	0.61	0.104	0.5534	1.63E-01	0.79
	48	2.39	1.04	0.104	0.8316	5.03E-03	2.30
	72	3.49	1.18	0.093	0.9064	1.10E-03	2.96
	96	4.15	1.22	0.072	0.9460	3.97E-04	3.40

Table S12. The Logit function fitting parameters and statistics, mean effect concentration and its negative logarithm for the Pb-Zn-Cd-Cu-Mn quinary mixture.

Ray	Time/h	Parameters				EC_{50} (mol/L)	pEC_{50}
		α	β	RMSE	R		
R1	12	1.43	1.27	0.038	0.7239	7.48E-02	1.13
	24	3.49	1.69	0.024	0.9683	8.61E-03	2.07
	48	4.65	1.87	0.044	0.9578	3.26E-03	2.49
	72	5.17	1.8	0.064	0.9498	1.34E-03	2.87
	96	6.25	2.03	0.060	0.9666	8.34E-04	3.08
R2	12	0.8	1.02	0.028	0.7696	1.64E-01	0.78
	24	4.69	2.06	0.032	0.9575	5.29E-03	2.28
	48	6.13	2.28	0.053	0.9650	2.05E-03	2.69
	72	6.65	2.22	0.073	0.9572	1.01E-03	3.00
	96	7.74	2.43	0.061	0.9752	6.53E-04	3.19
R3	12	1.74	1.16	0.028	0.8285	3.16E-02	1.50
	24	4.62	1.91	0.024	0.9564	3.81E-03	2.42
	48	5.19	1.83	0.045	0.9473	1.46E-03	2.84
	72	6.15	1.94	0.077	0.9219	6.76E-04	3.17
	96	8.04	2.43	0.087	0.9312	4.91E-04	3.31
R4	12	1.28	1.02	0.045	0.7132	5.56E-02	1.25
	24	5.11	2.05	0.063	0.8931	3.22E-03	2.49
	48	5.99	2.05	0.069	0.9420	1.20E-03	2.92
	72	7.68	2.4	0.093	0.9430	6.31E-04	3.20
	96	9.31	2.82	0.085	0.9586	5.00E-04	3.30
R5	12	8.49	3.16	0.029	0.9378	2.06E-03	2.69
	24	13.63	4.67	0.035	0.9593	1.21E-03	2.92
	48	12.05	3.94	0.051	0.9581	8.74E-04	3.06
	72	11.51	3.6	0.076	0.9413	6.35E-04	3.20
	96	14.21	4.3	0.086	0.9478	4.96E-04	3.30

Table S12. Continued.

R6	12	4.07	2.00	0.057	0.6550	9.23E-03	2.04
	24	7.10	2.70	0.063	0.8789	2.35E-03	2.63
	48	7.02	2.40	0.076	0.9304	1.19E-03	2.93
	72	7.99	2.52	0.090	0.9408	6.75E-04	3.17
	96	10.99	3.33	0.101	0.9511	5.01E-04	3.30
R7	12	0.01	0.63	0.019	0.8373	9.64E-01	0.02
	24	4.71	2.20	0.027	0.9521	7.23E-03	2.14
	48	5.50	2.05	0.051	0.9552	2.08E-03	2.68
	72	5.73	1.89	0.073	0.9428	9.30E-04	3.03
	96	7.02	2.19	0.059	0.9712	6.23E-04	3.21

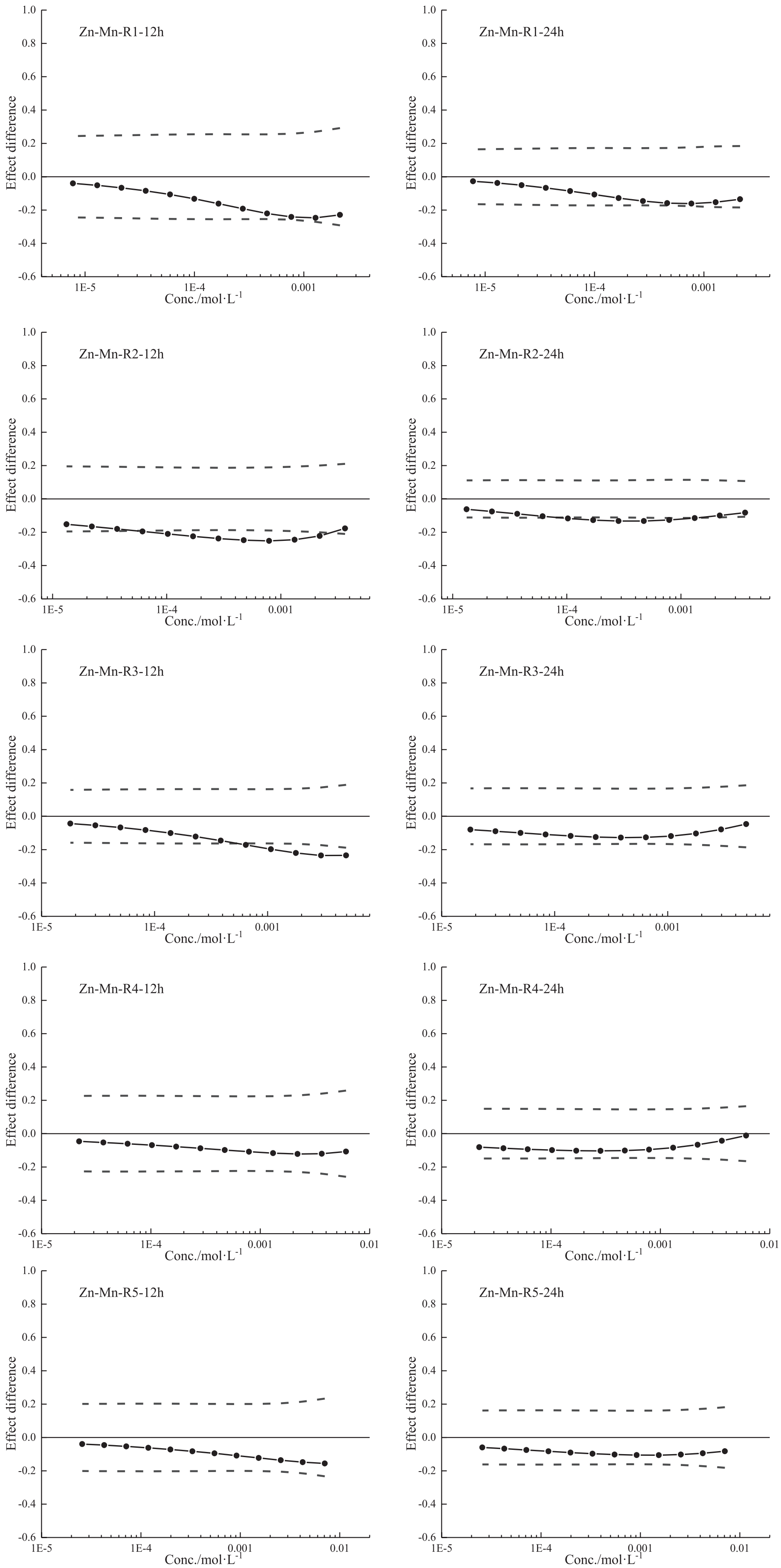

Fig. S1. Plot of RTZF curves of Zn-Mn binary mixture on *C. pyrenoidosa*.

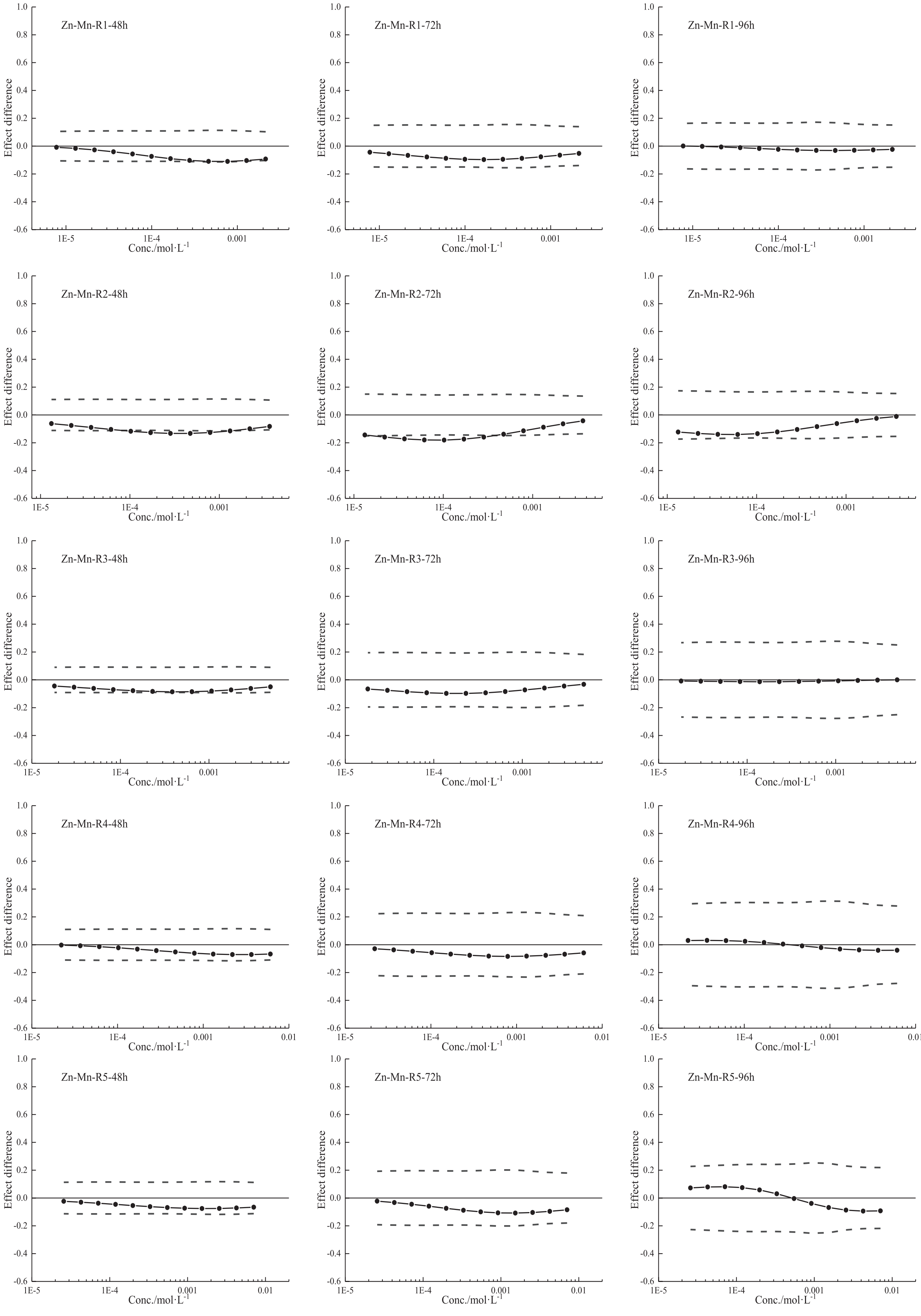

Fig. S1. Continued.

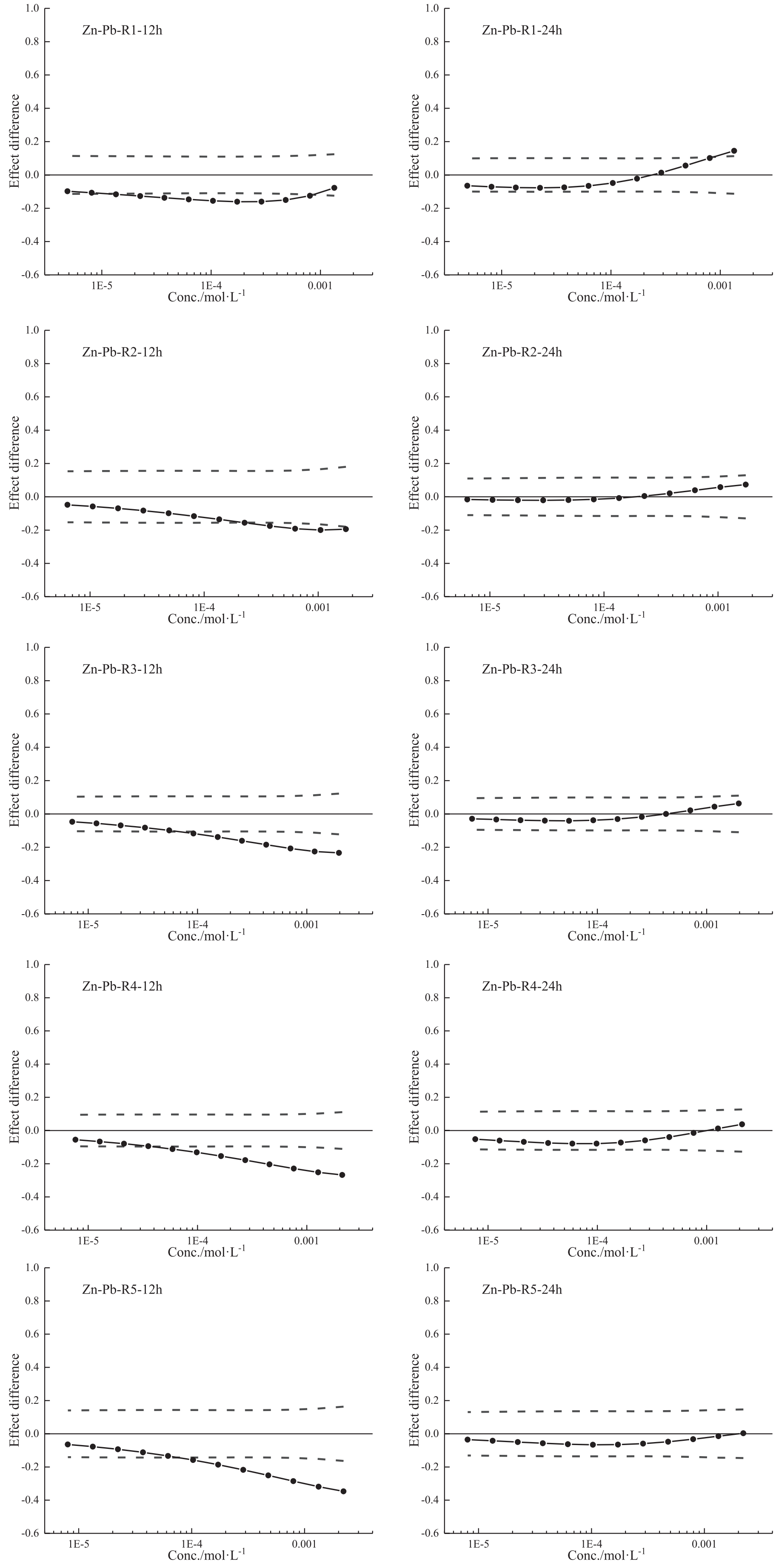

Fig. S2. Plot of RTZF curves of Zn-Pd binary mixture on *C. pyrenoidosa.*

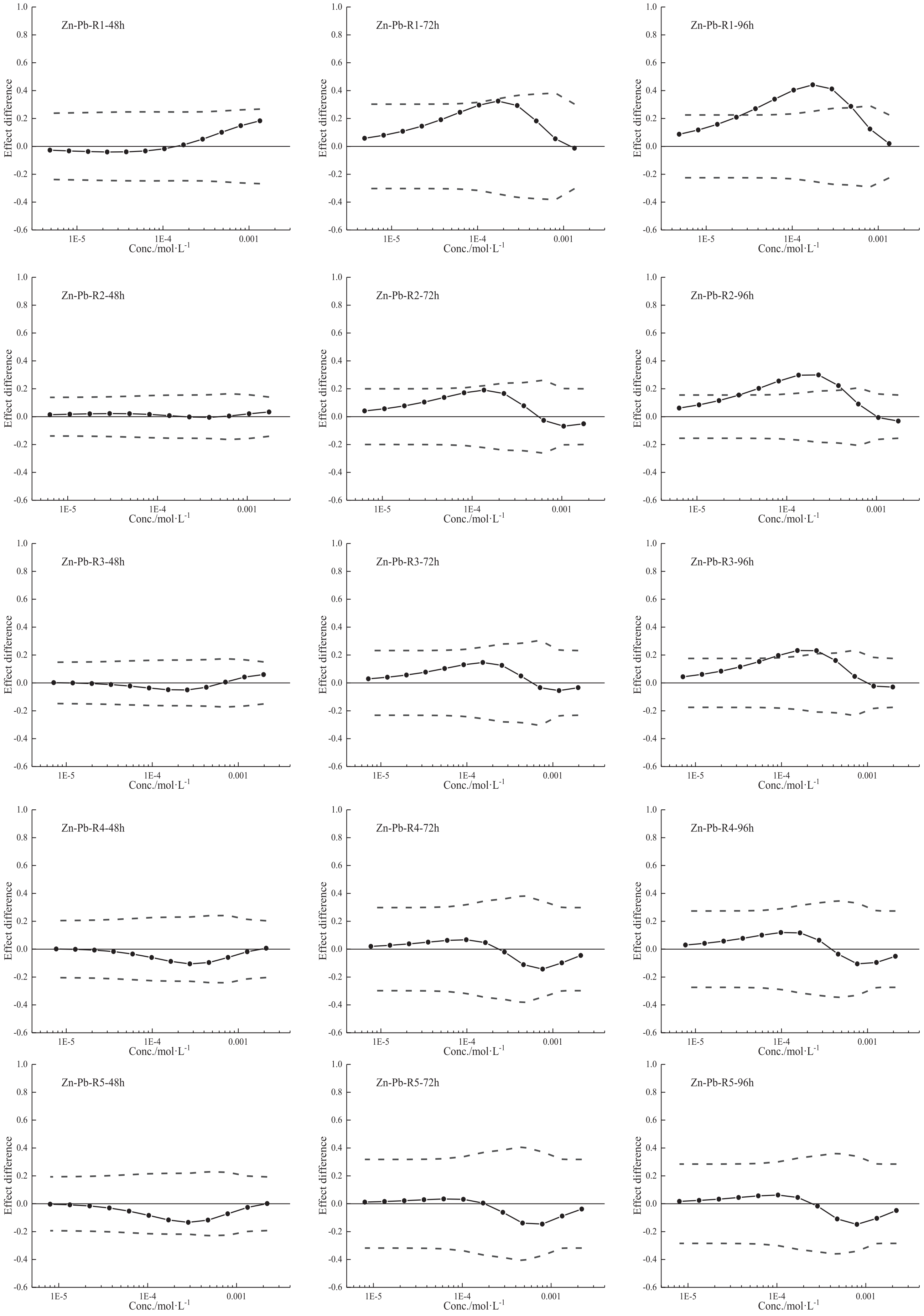

Fig. S2. Continued.

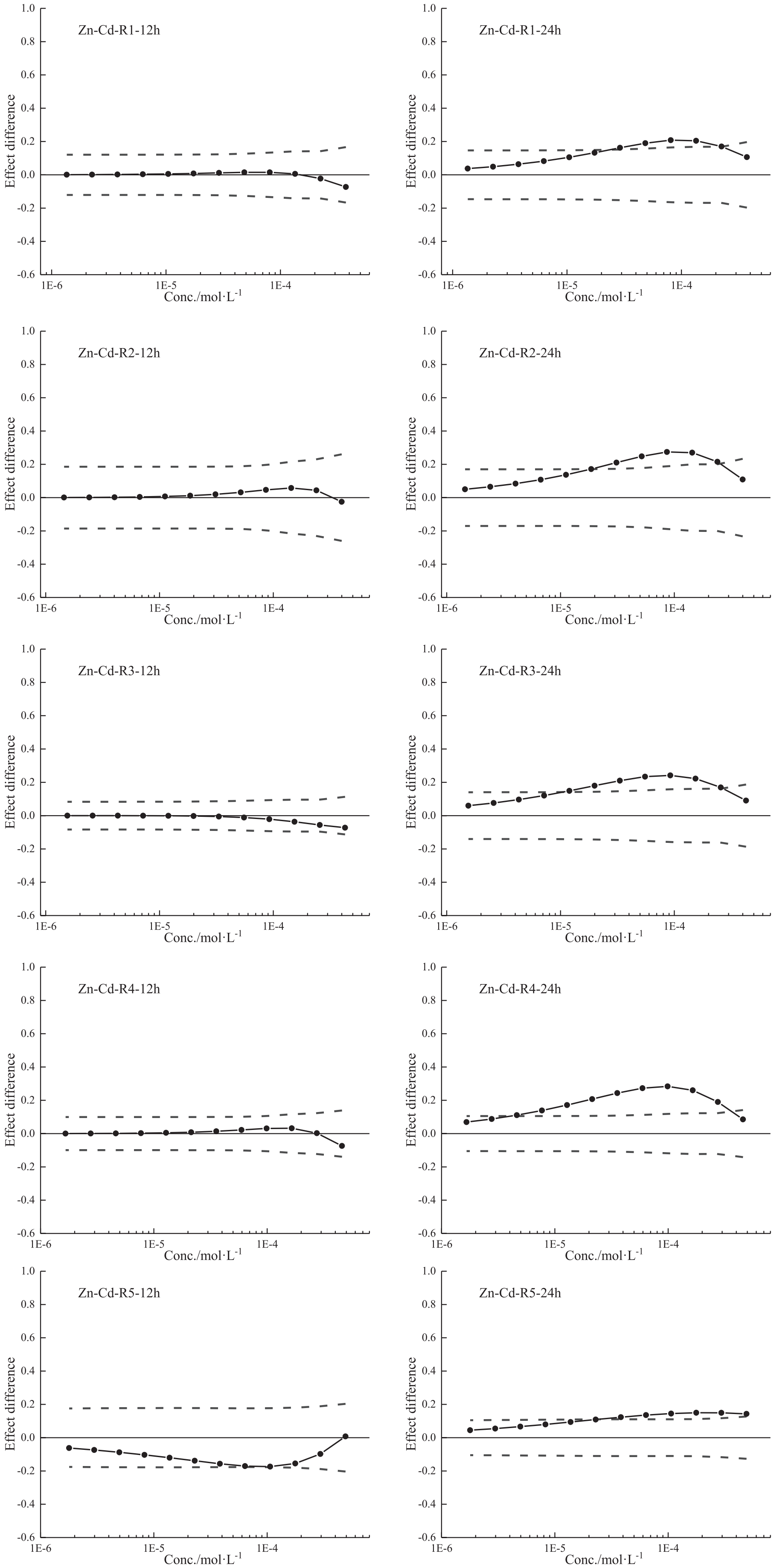

Fig. S3. Plot of RTZF curves of Zn-Cd binary mixture on *C. pyrenoidosa.*

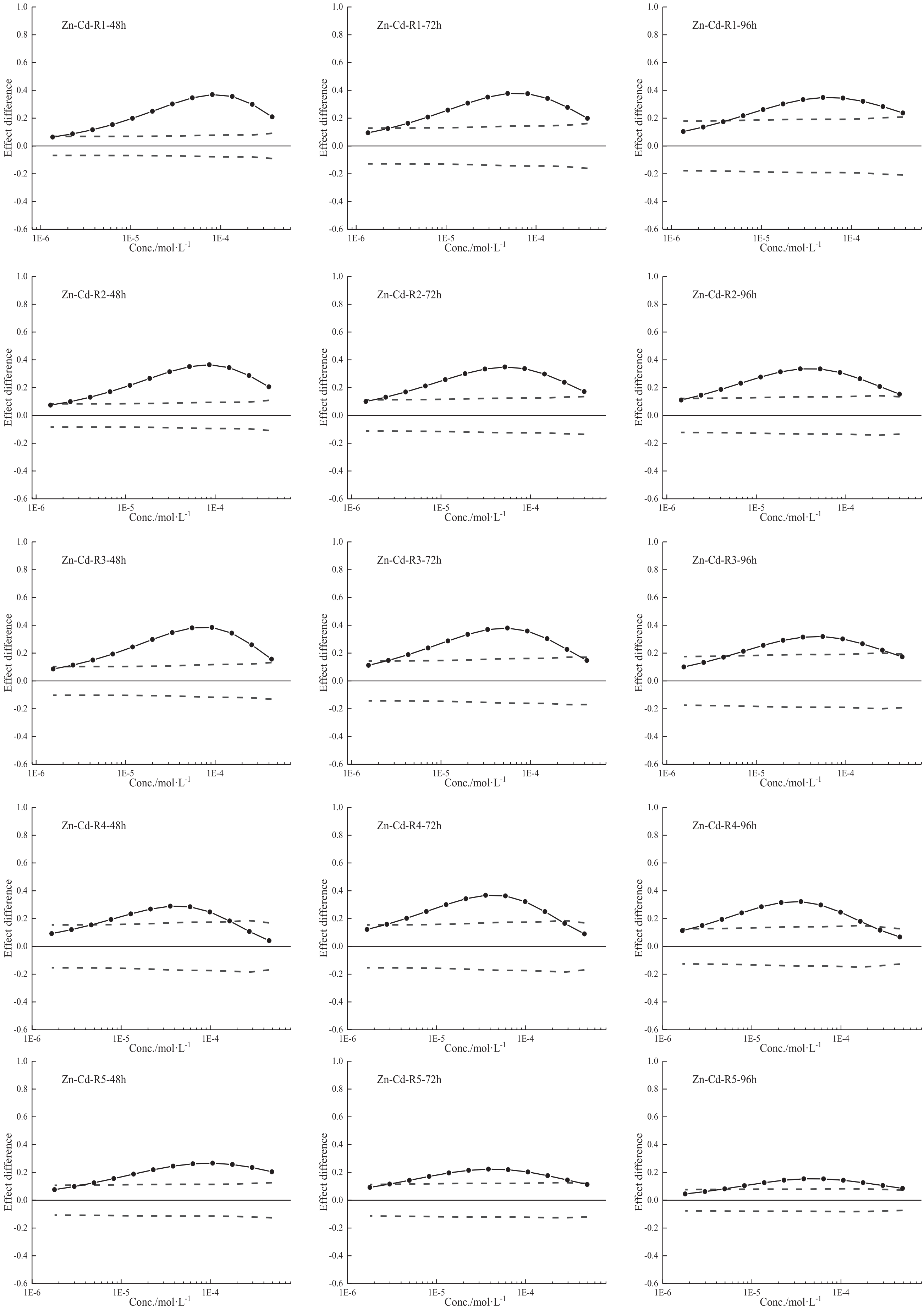

Fig. S3. Continued.

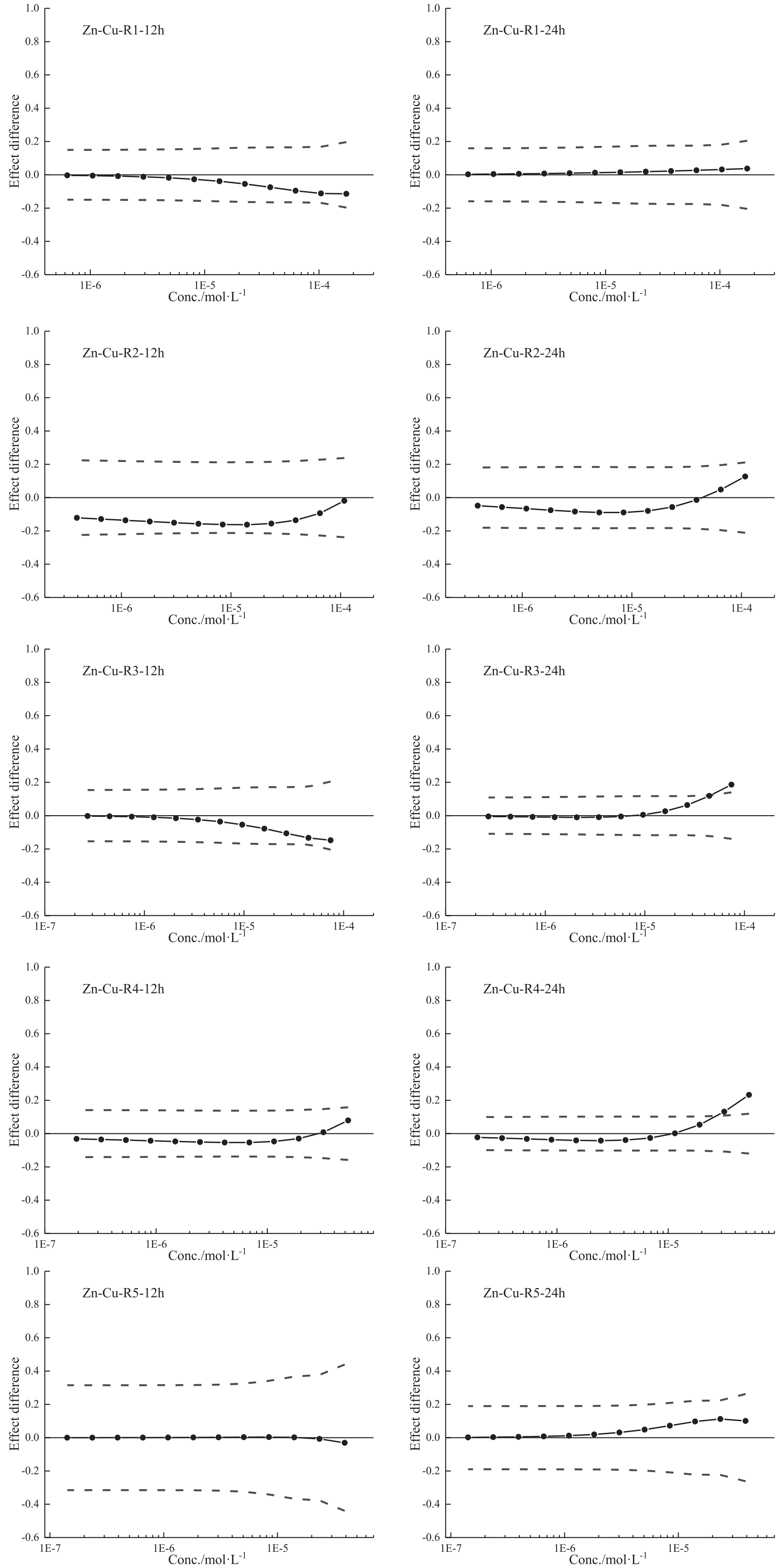

Fig. S4. Plot of RTZF curves of Zn-Cu binary mixture on *C. pyrenoidosa.*

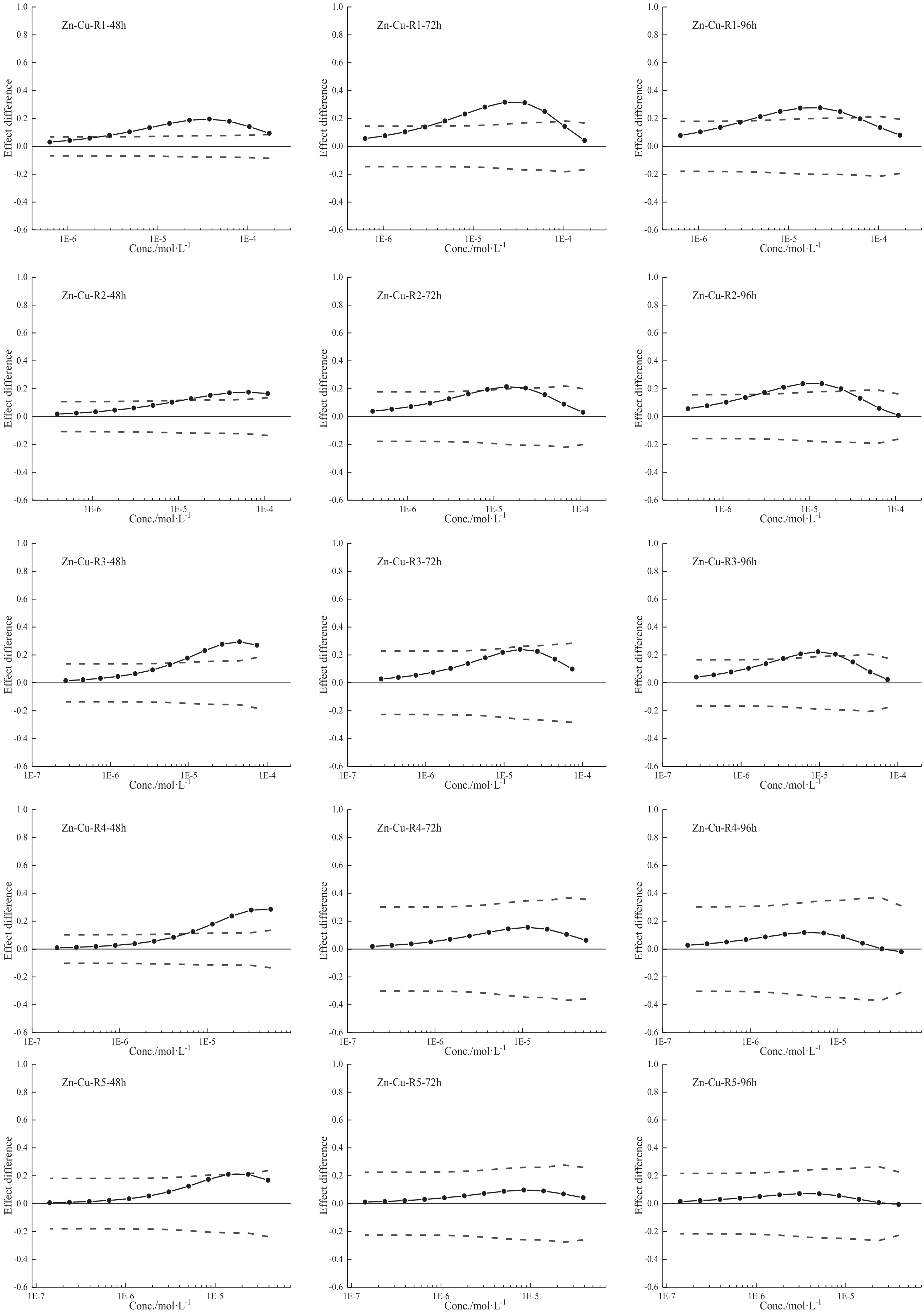

Fig. S4. Continued.

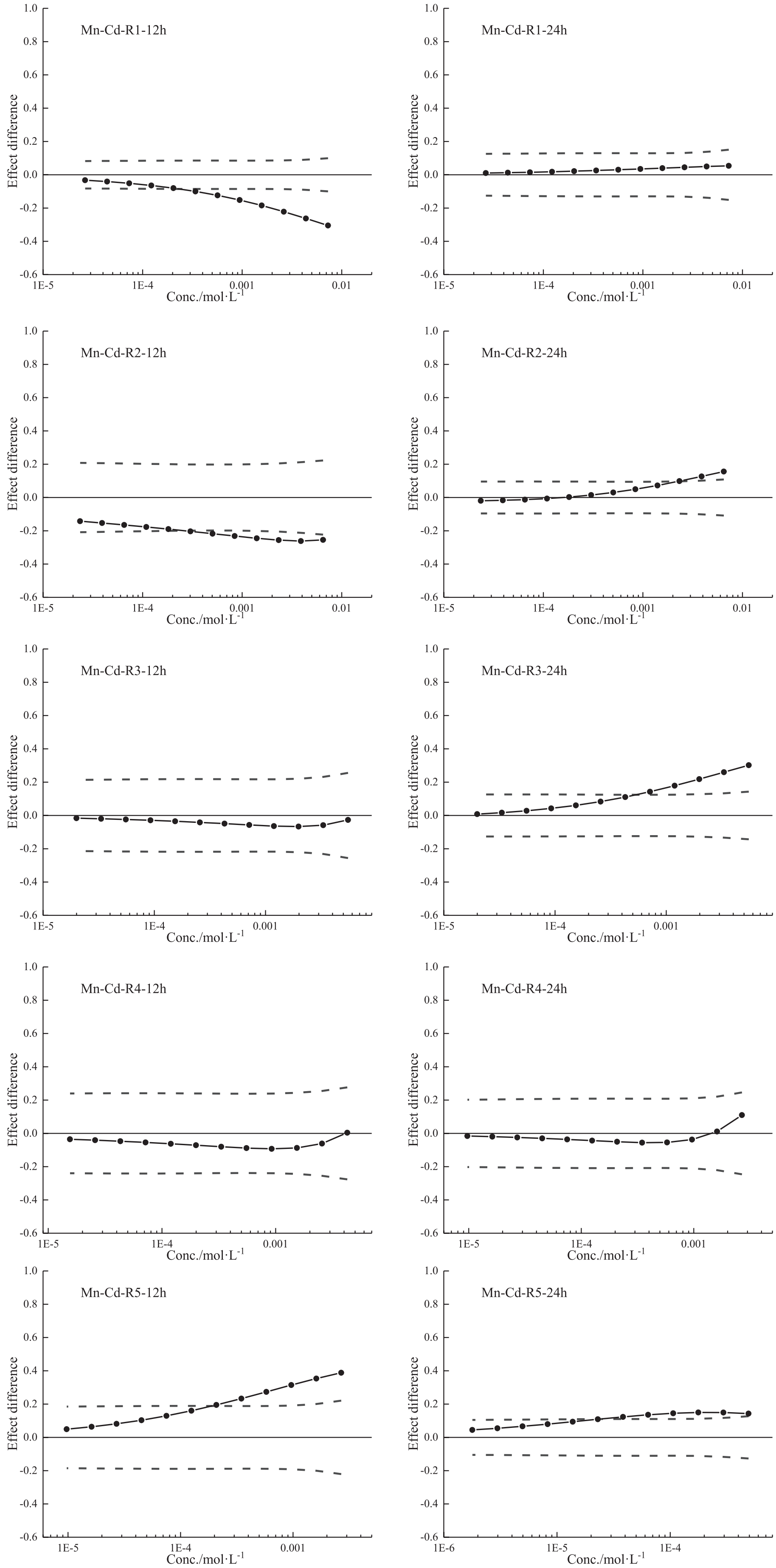

Fig. S5. Plot of RTZF curves of Mn-Cd binary mixture on *C. pyrenoidosa*.

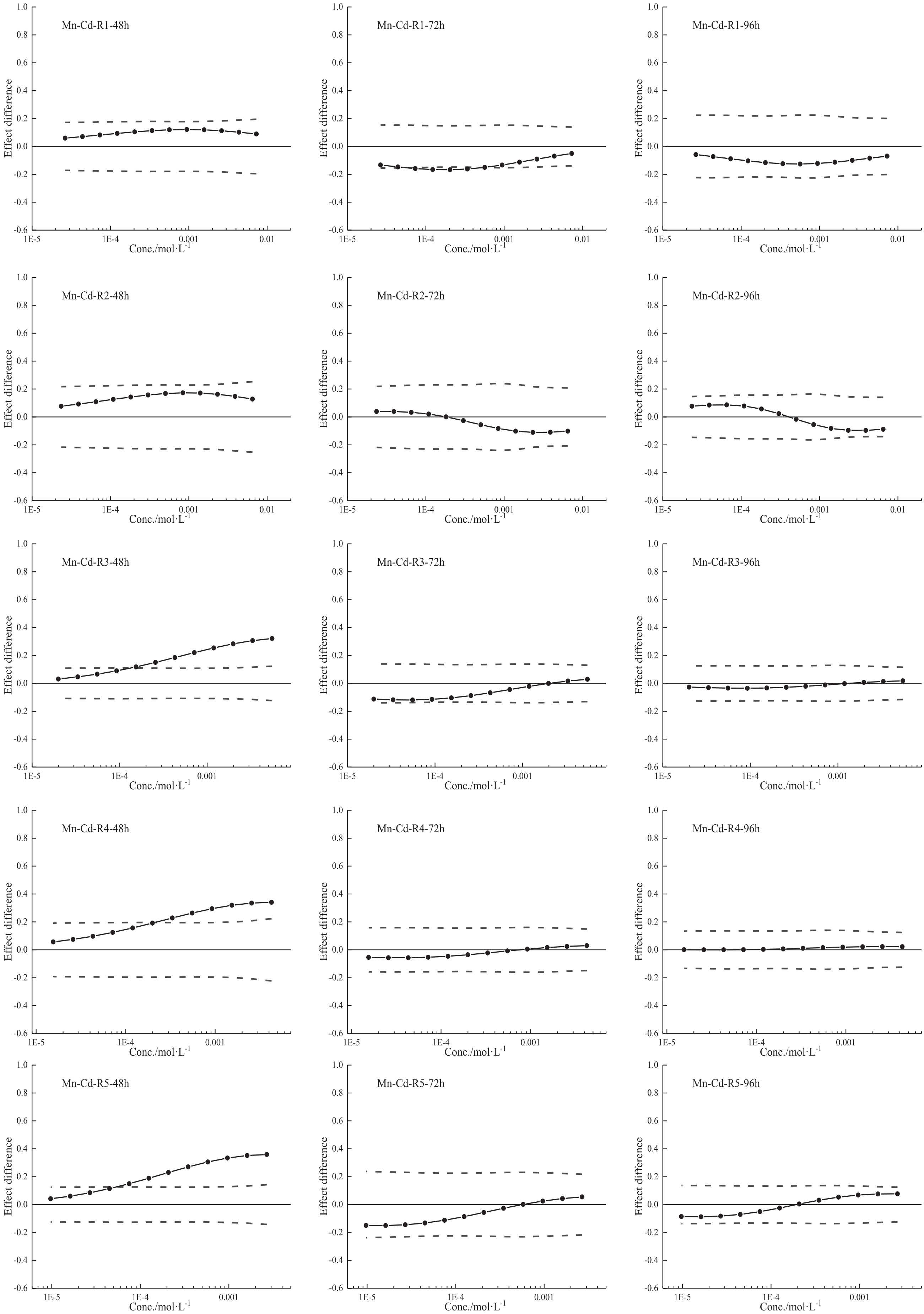

Fig. S5. Continued.

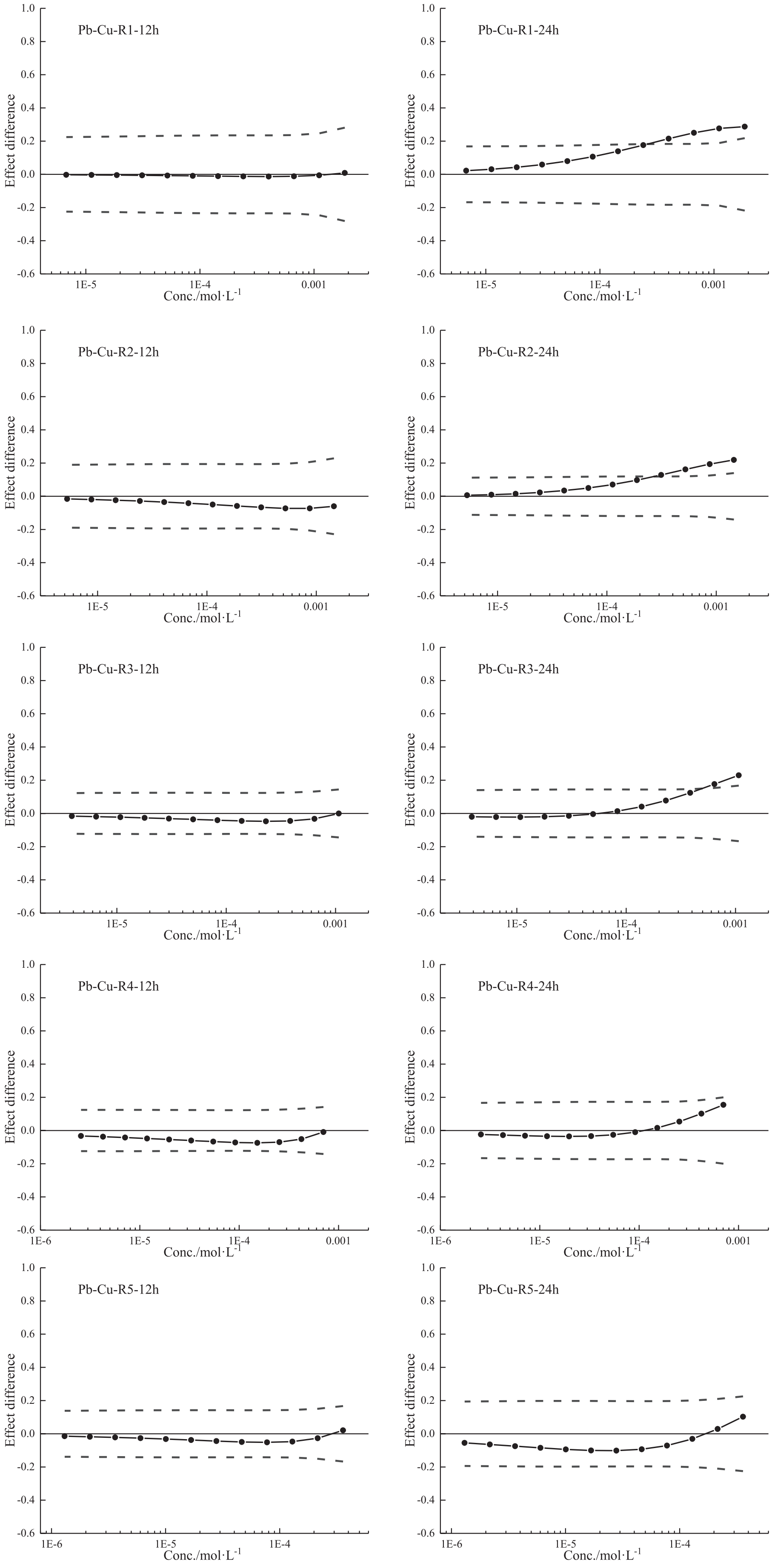

Fig. S6. Plot of RTZF curves of Pb-Cu binary mixture on *C. pyrenoidosa.*

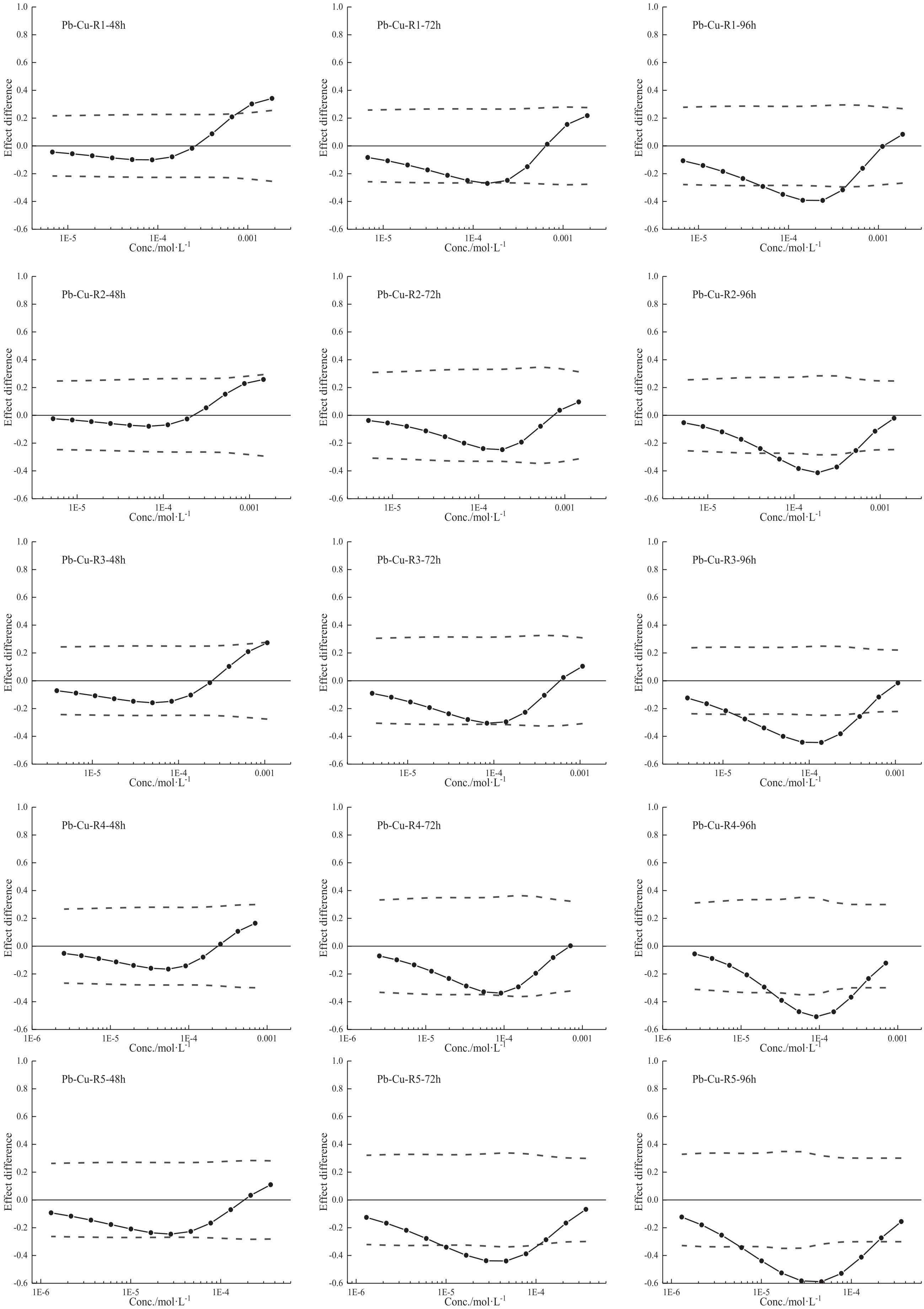

Fig. S6. Continued.

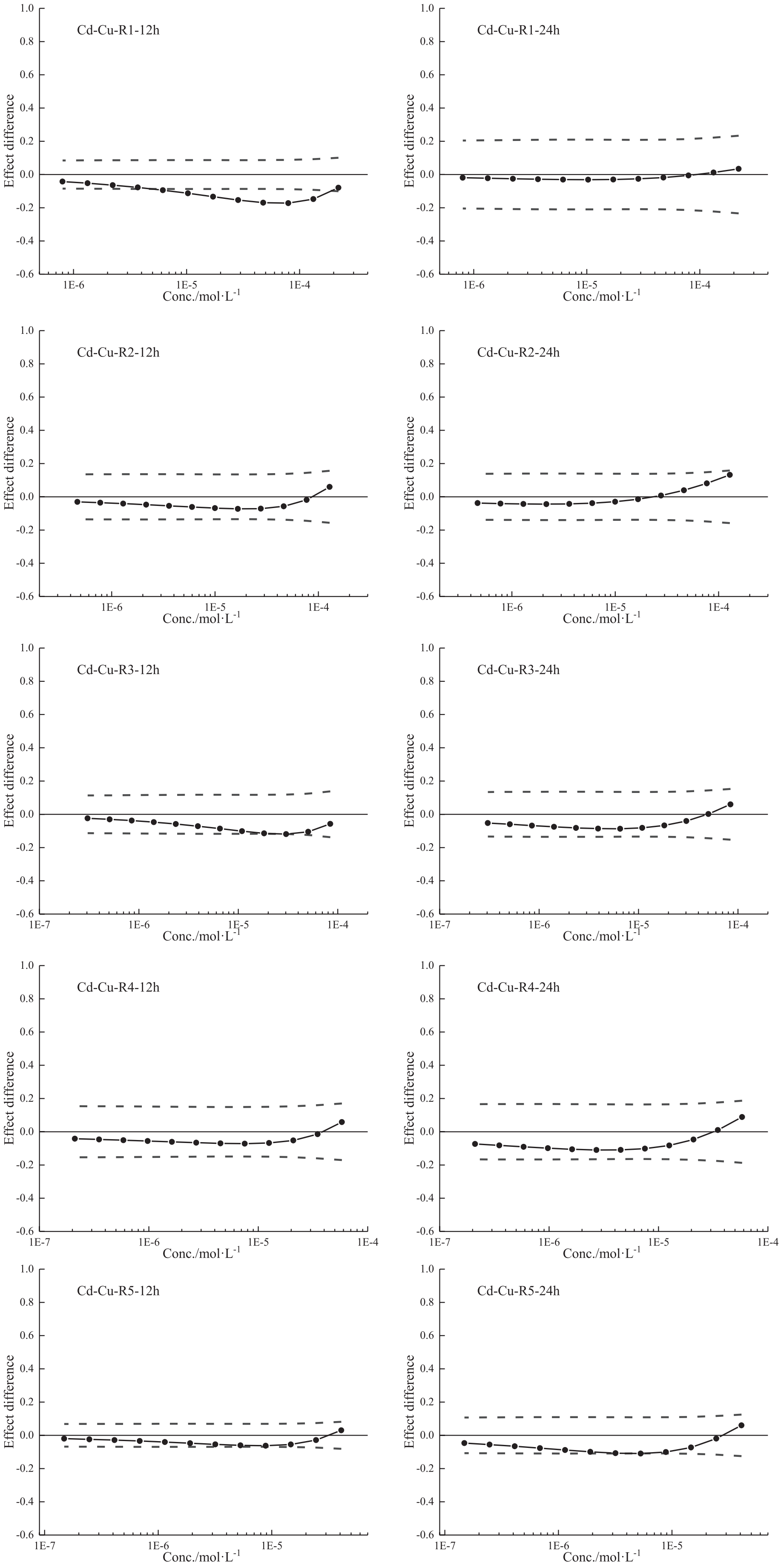

Fig. S7. Plot of RTZF curves of Cd-Cu binary mixture on *C. pyrenoidosa.*

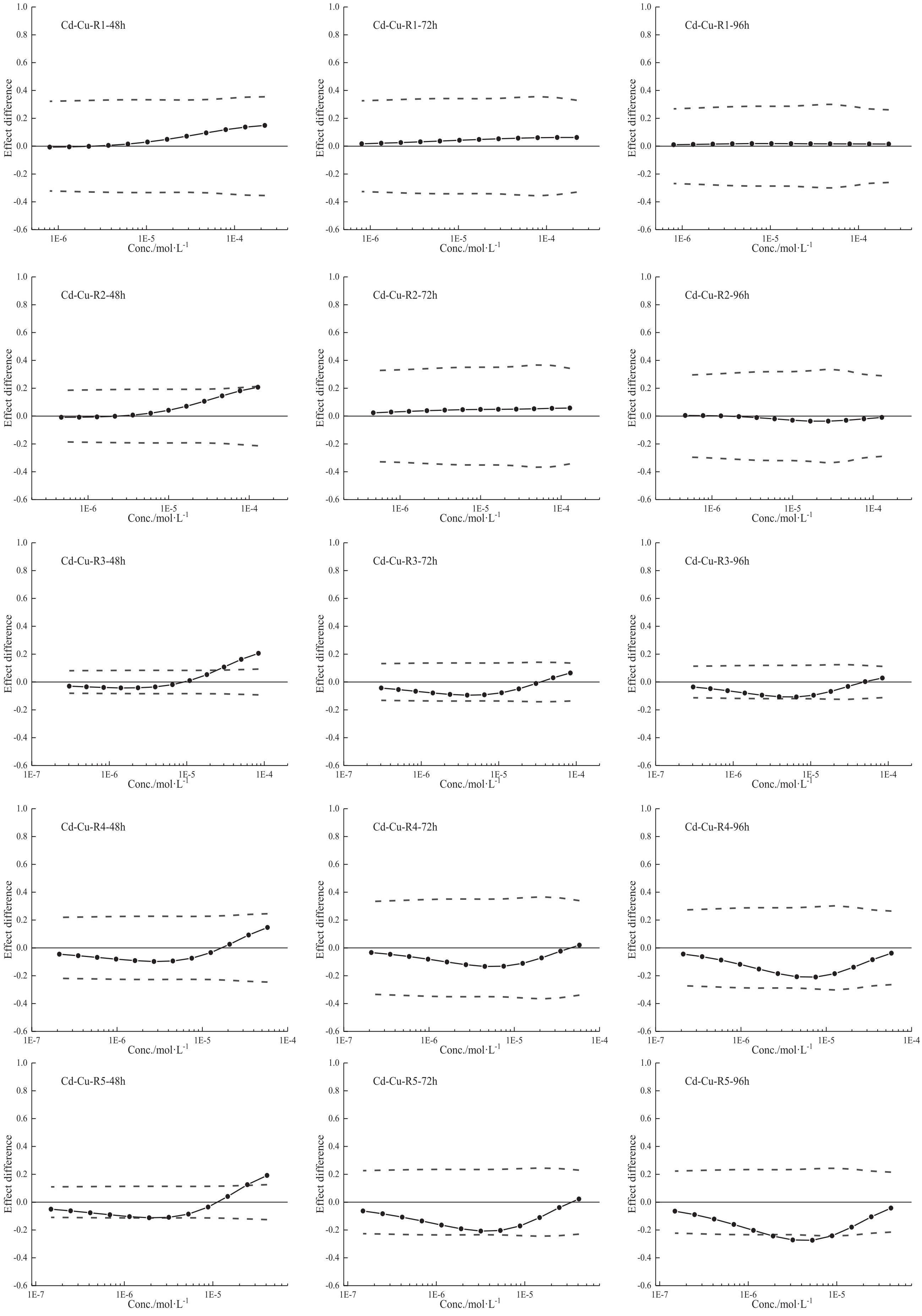

Fig. S7. Continued.

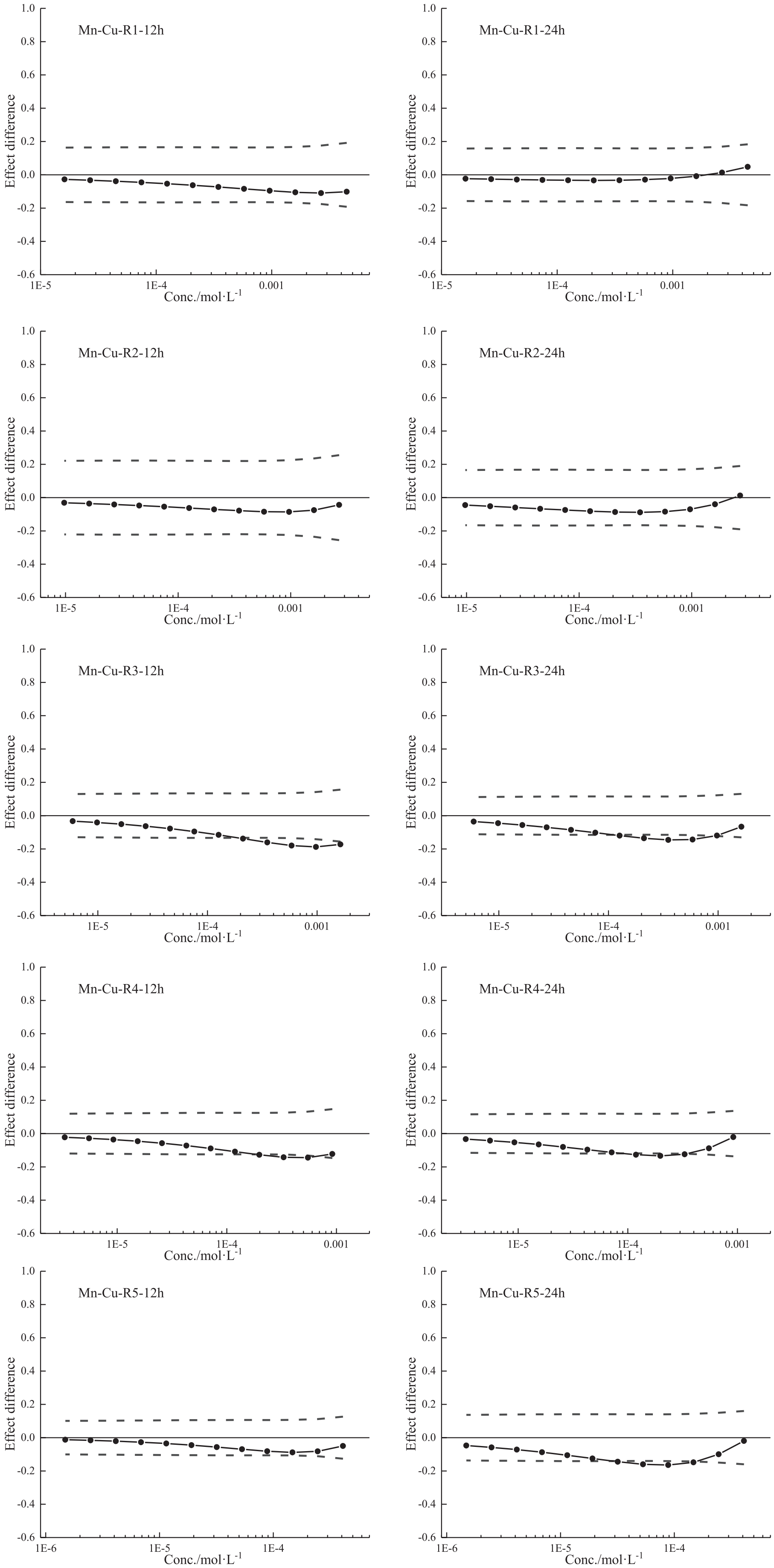

Fig. S8. Plot of RTZF curves of Mn-Cu binary mixture on *C. pyrenoidosa*.

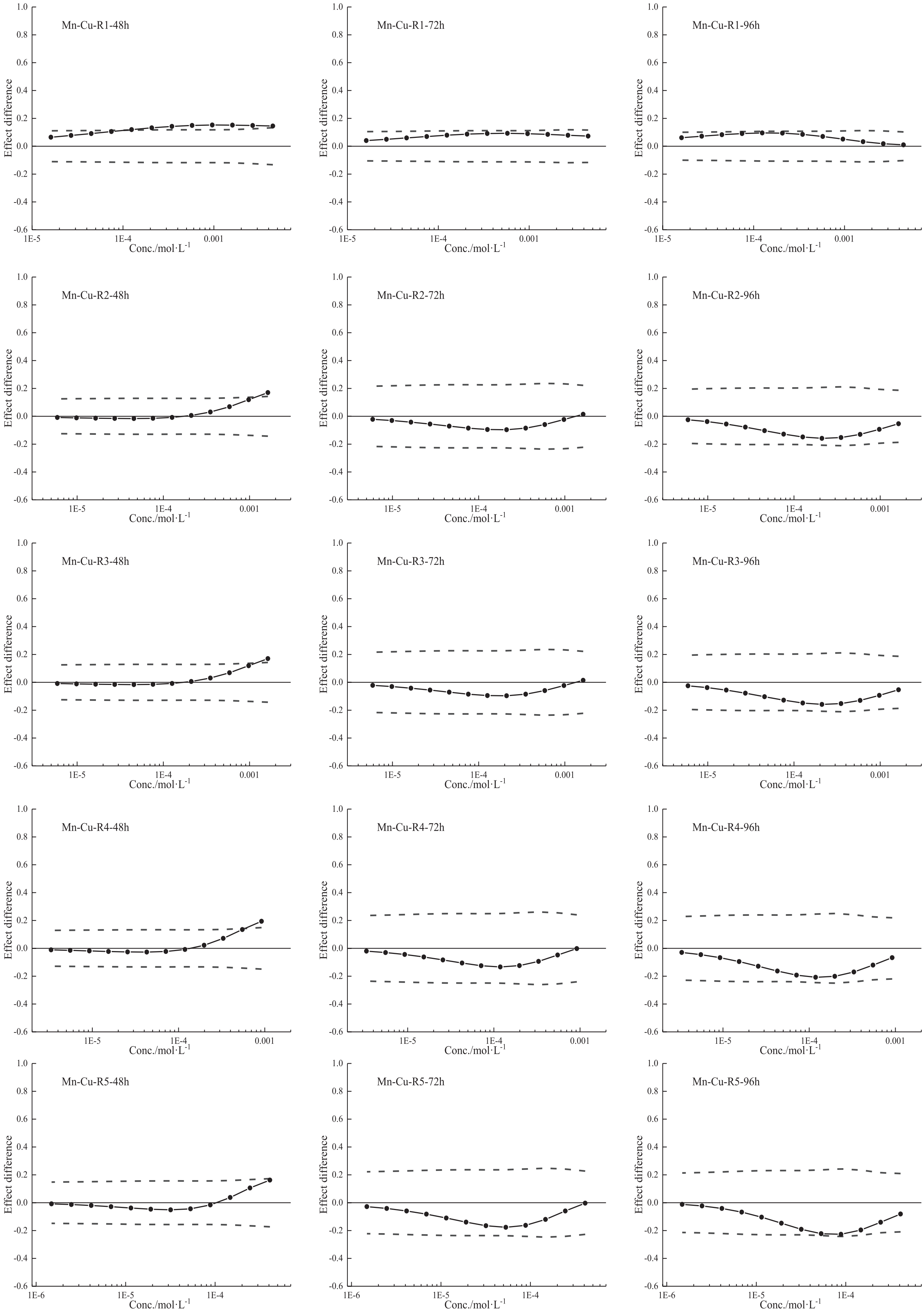

Fig. S8. Continued.

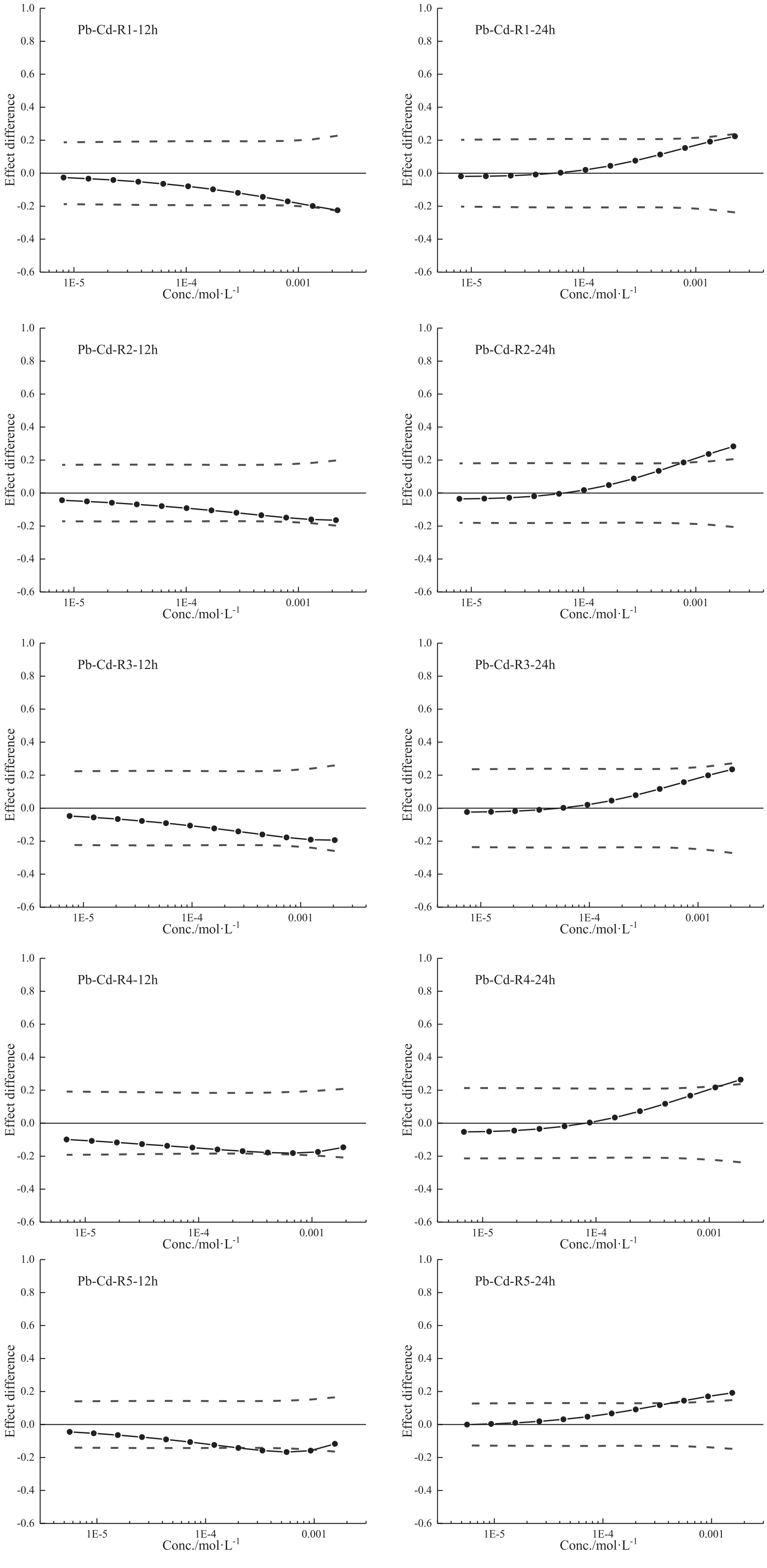

Fig. S9. Plot of RTZF curves of Pb-Cd binary mixture on *C. pyrenoidosa.*

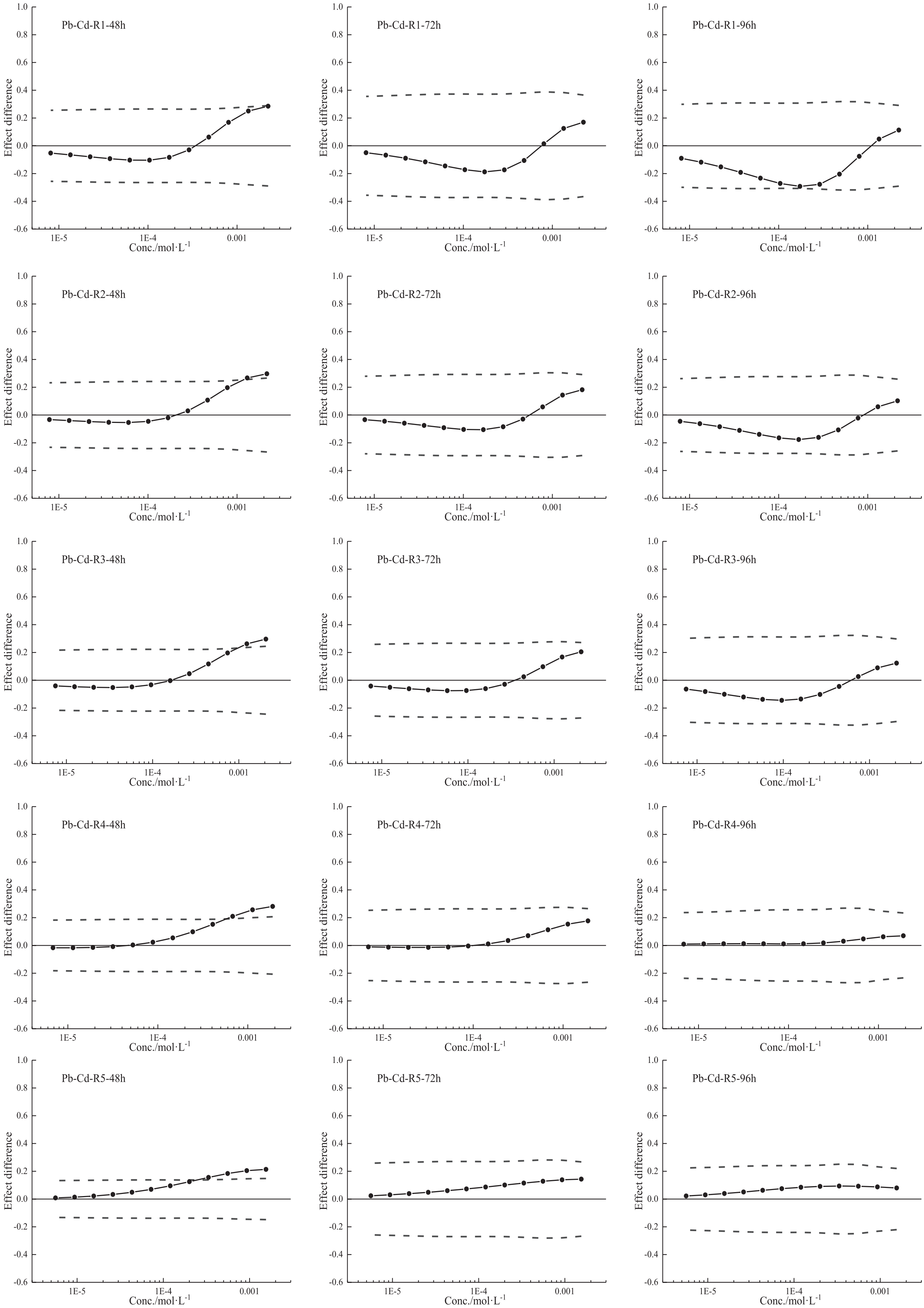

Fig. S9. Continued.

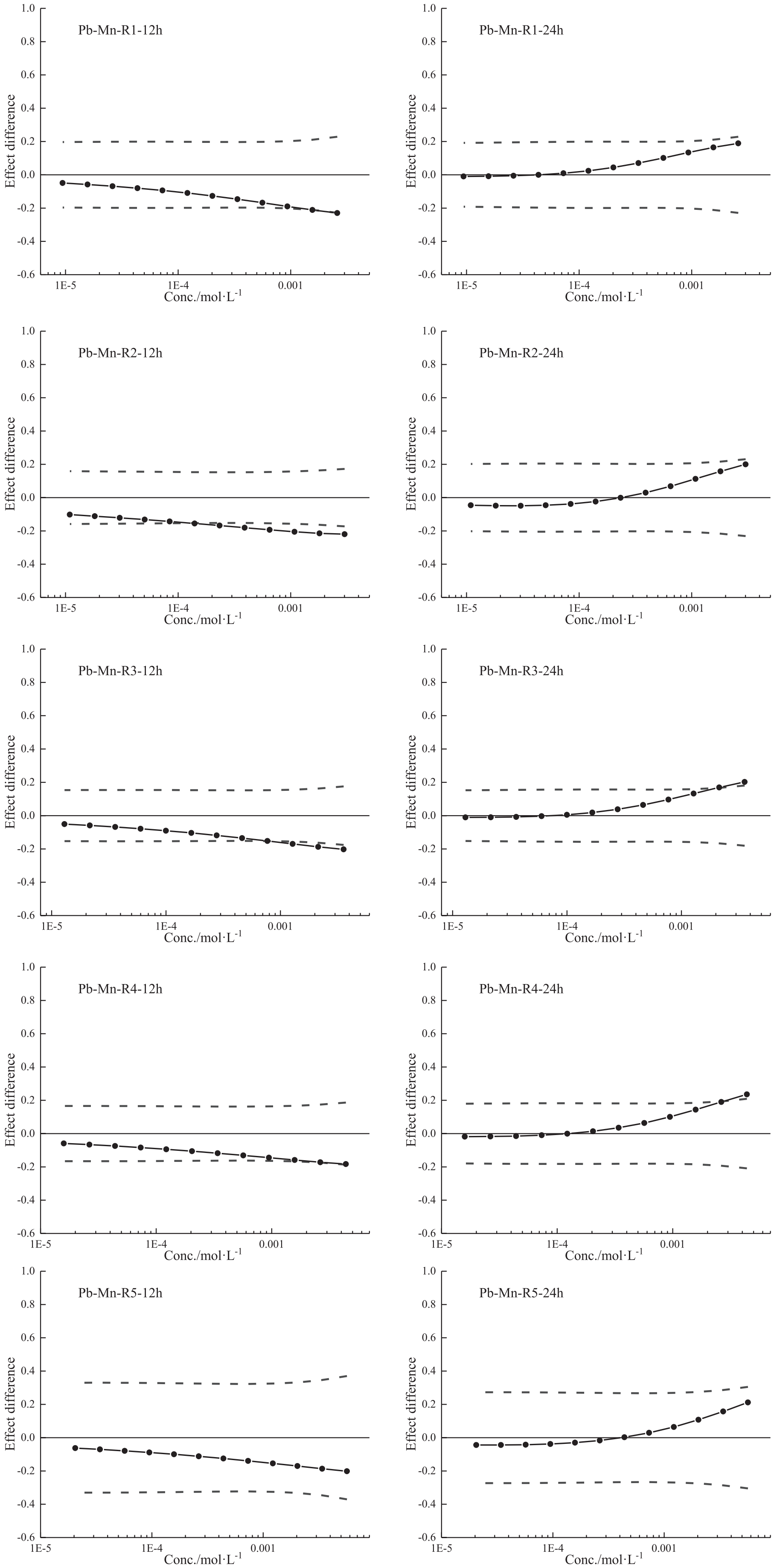

Fig. S10. Plot of RTZF curves of Pb-Mn binary mixture on *C. pyrenoidosa.*

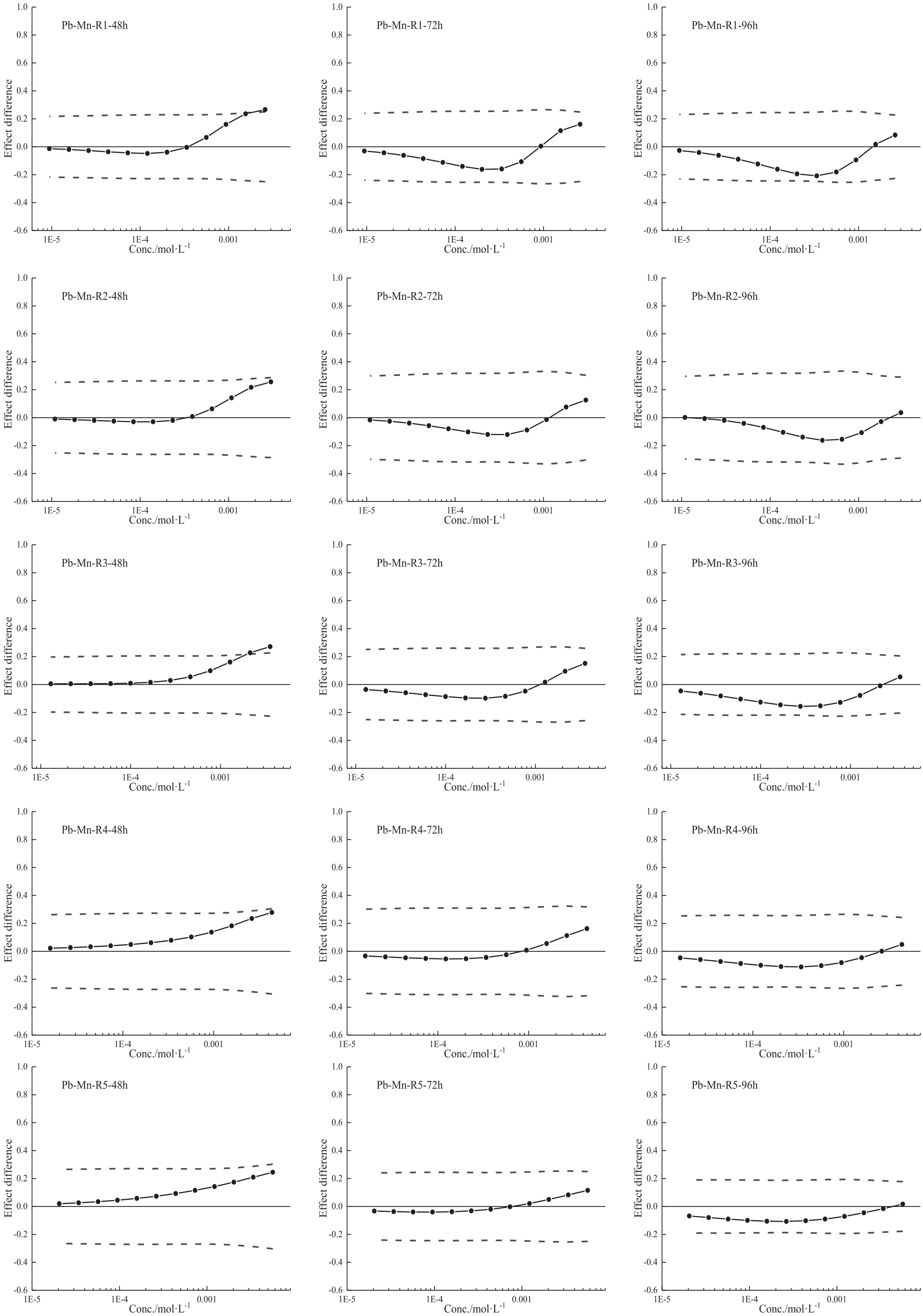

Fig. S10. Continued.

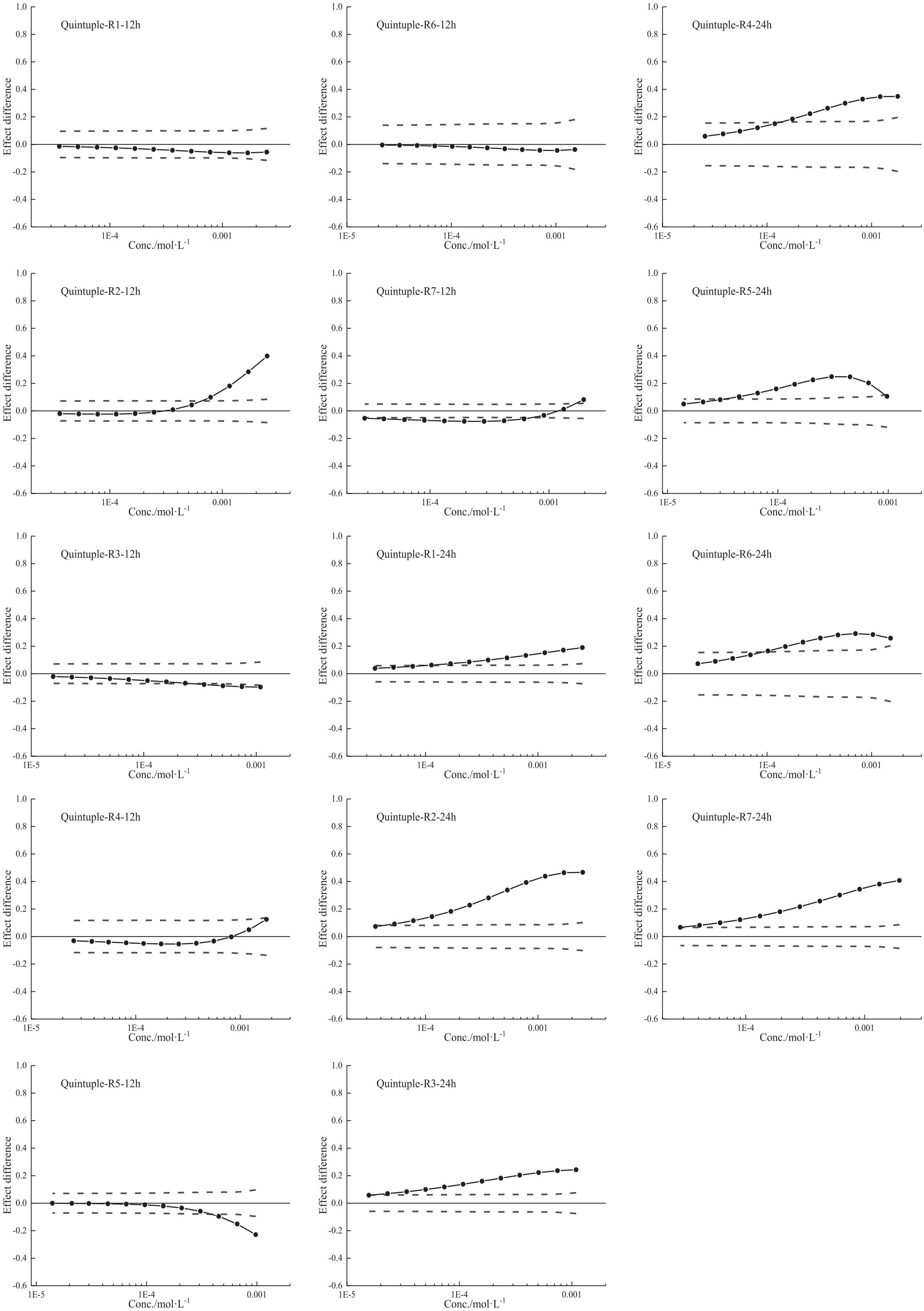

Fig. S11. Plot of RTZF curves of quinary mixture on *C. pyrenoidosa.*

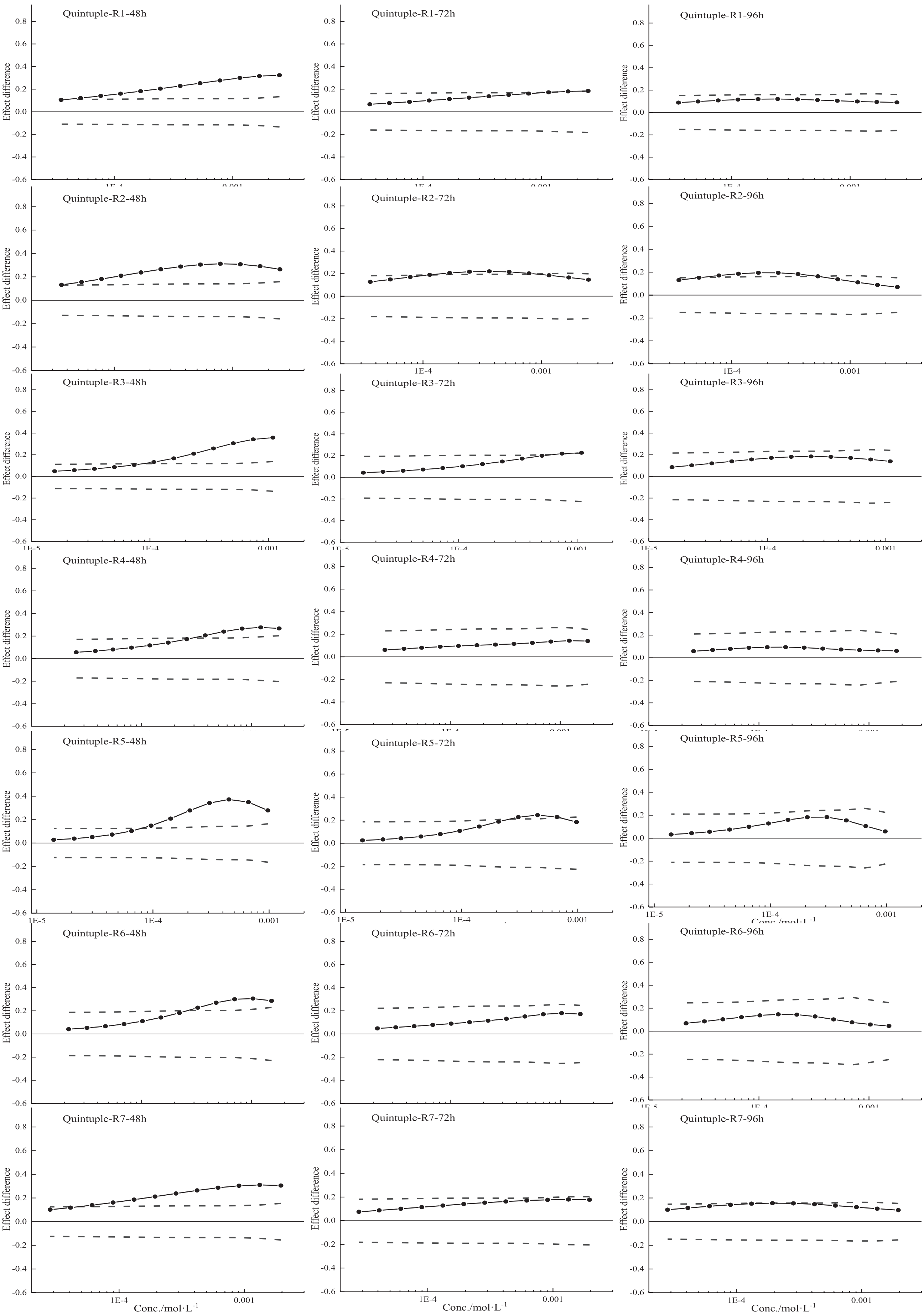

Fig. S11. Continued.